6

MODELING ADSORPTION OF METALS AND METALLOIDS BY SOIL COMPONENTS

S. GOLDBERG

George E. Brown, Jr., Salinity Laboratory, USDA-ARS, Riverside, California

L. J. CRISCENTI

Sandia National Laboratories, Albuquerque, New Mexico

Biophysico-Chemical Processes of Heavy Metals and Metalloids in Soil Environments, Edited by Antonio Violante, Pan Ming Huang, and Geoffrey Michael Gadd

6.1. INTRODUCTION

Adsorption is the accumulation of a chemical species at the interface between a solid phase and a fluid phase. In adsorption, a two-dimensional molecular surface structure is retained. Adsorption processes in soils have been described using a variety of approaches. Empirical adsorption models provide descriptions of experimental adsorption data without any theoretical basis. Chemical adsorption models, on the other hand, provide a molecular description of adsorption reactions.

The purpose of this chapter is to present several of the most common models used to describe metal and metalloid ion adsorption by soil components. Empirical models used in soil chemistry are described and their limitations discussed. Common chemical models used to describe metal adsorption on soil minerals are described and their advantages over empirical approaches discussed. Methods for obtaining model parameters are provided. Methods for establishing adsorption mechanisms and surface speciation are addressed. Limitations and approximations in the application of chemical models to natural systems are presented.

6.2. DESCRIPTION OF MODELS

6.2.1. Empirical Models—Historical Development

Adsorption reactions by soil minerals and soils have been described historically using empirical adsorption isotherm equations. As their name implies, it is understood that they are used for experiments at constant temperature, which unless indicated, otherwise is standard temperature, $T = 298$ K. An adsorption isotherm is a plot of the concentration adsorbed to a solid surface versus the concentration in aqueous solution for different total concentrations of a chemical species. Typically, adsorption isotherm equations are very good at describing experimental data, despite their lack of theoretical basis. Popularity of these equations stems in part from their simplicity and from the ease of estimation of their adjustable parameters.

6.2.1.1. Distribution Coefficient The simplest and most widely used adsorption isotherm equation is a linear function. This adsorption isotherm equation is

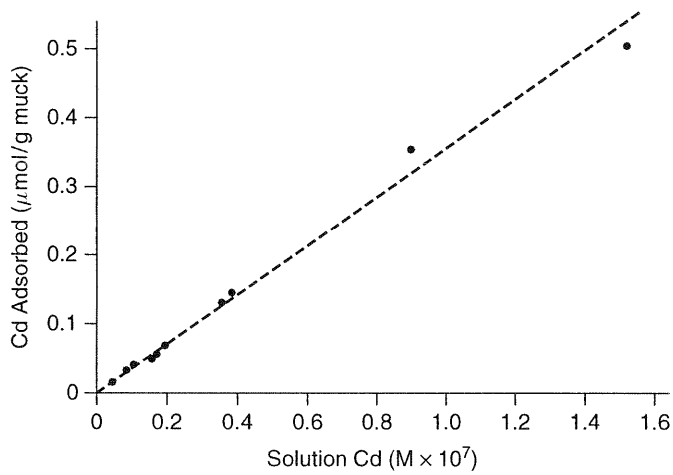

Figure 6.1. Linear adsorption of cadmium by the organic component of a muck soil. (From Turner et al., 1984.)

written in terms of the distribution coefficient, K_d:

$$x = K_d c \tag{6.1}$$

where x is the amount of chemical species adsorbed per unit mass of solid and c is the equilibrium solution concentration of the chemical species. Because of the linear assumption, the distribution coefficient usually describes adsorption data only over a very restricted solution concentration range. Figure 6.1 shows the ability of the distribution coefficient to describe linear adsorption of cadmium by the organic component of a muck soil (Turner et al., 1984). In this example, adsorption is linear over the solution metal concentration range investigated.

6.2.1.2. Freundlich Adsorption Isotherm Equation The Freundlich adsorption isotherm equation is the oldest of the nonlinear isotherms, and its use implies heterogeneity of adsorption sites. The Freundlich isotherm equation is

$$x = K c^{\beta} \tag{6.2}$$

where K is an affinity parameter and β is a dimensionless heterogeneity parameter; the smaller the value of β, the greater the heterogeneity (Kinniburgh, 1985). The Freundlich equation reduces to a linear adsorption isotherm when $\beta = 1$. Although the Freundlich adsorption isotherm is strictly valid only for metal adsorption at low aqueous metal concentration (Sposito, 1984), it has often been used to describe metal adsorption by soils over the entire metal concentration range investigated. The Freundlich equation does not obey Henry's law at low metal concentration, nor does it reach an adsorption maximum at high metal concentration (Kinniburgh, 1985). The ability of the Freundlich adsorption isotherm

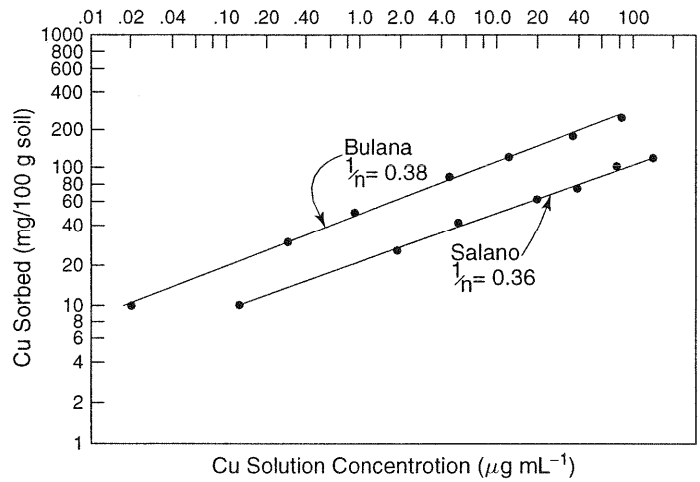

Figure 6.2. Fit of the Freundlich adsorption isotherm equation to copper adsorption by two soils. (From Kurdi and Doner, 1983.)

to describe metal adsorption data is indicated in Figure 6.2 for copper adsorption by two California soils (Kurdi and Doner, 1983).

6.2.1.3. Langmuir Adsorption Isotherm Equation The Langmuir adsorption isotherm equation was developed originally to describe gas adsorption onto clean surfaces and can be derived theoretically based on rates of evaporation and condensation (Adamson, 1976). The Langmuir adsorption isotherm equation is

$$x = \frac{x_m K c}{1 + K c} \tag{6.3}$$

where x_m is the maximum adsorption of chemical species per unit mass of solid and K is an affinity parameter related to the bonding energy of the species to the surface. The Langmuir isotherm is derived assuming a finite number of uniform adsorption sites and the absence of lateral interaction between adsorbed species. Despite the fact that these assumptions are violated in soils, the Langmuir equation has often been used to describe metal adsorption reactions on soil minerals and soils. In many studies, the Langmuir isotherm equation is only able to describe adsorption for low solution metal concentrations. A successful application of the Langmuir isotherm equation is presented in Figure 6.3 for adsorption of copper by a calcareous soil (Cavallaro and McBride, 1978).

6.2.1.4. Multisite Langmuir Adsorption Isotherm Equation The multisite Langmuir adsorption isotherm equation was formulated for the simultaneous adsorption of a gas by more than one type of surface site. The multisite Langmuir

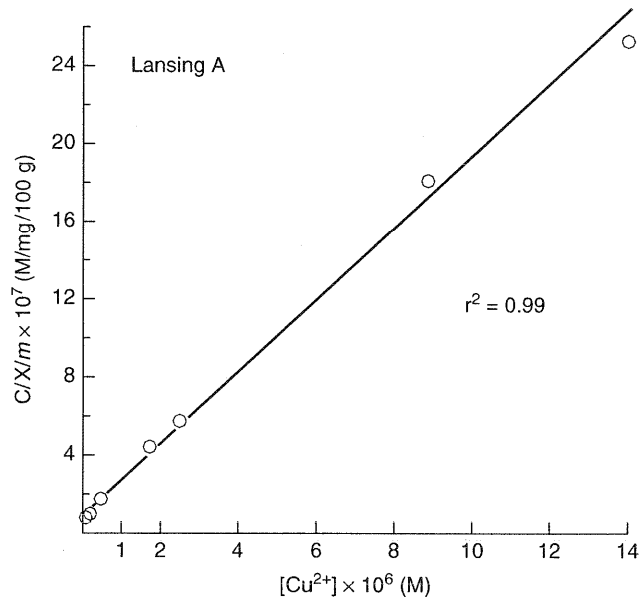

Figure 6.3. Fit of the Langmuir adsorption isotherm equation to copper adsorption by a soil. (From Cavallaro and McBride, 1978.)

isotherm equation is

$$x = \sum_{i=1}^{n} \frac{x_{m_i} K_i c}{1 + K_i c} \tag{6.4}$$

where n is the number of types of surface sites. Because of the increase in the number of adjustable parameters, the fit to metal adsorption data with the multisite Langmuir isotherm is often much improved over the single Langmuir isotherm. The high quality of fit obtained with the multisite Langmuir equation can be observed in Figure 6.4 for zinc adsorption by a Georgia soil (Shuman, 1975).

6.2.1.5. Limitations of the Empirical Approach Although theoretically impossible, the Langmuir adsorption isotherm equation can mathematically describe experimental data for a precipitation reaction (Veith and Sposito, 1977). Adherence of experimental data to an adsorption isotherm equation provides no information about the chemical reaction mechanism (Sposito, 1982). Any reaction process for which the distribution coefficient, K_d, is a finite, decreasing function of the amount adsorbed, x, and extrapolates to zero at a finite value of x, can be represented mathematically using a two-surface Langmuir adsorption isotherm equation (Sposito, 1982). Although adsorption isotherm equations are often excellent at describing metal adsorption, they must be considered simply as numerical relationships used to fit data. Independent experimental evidence

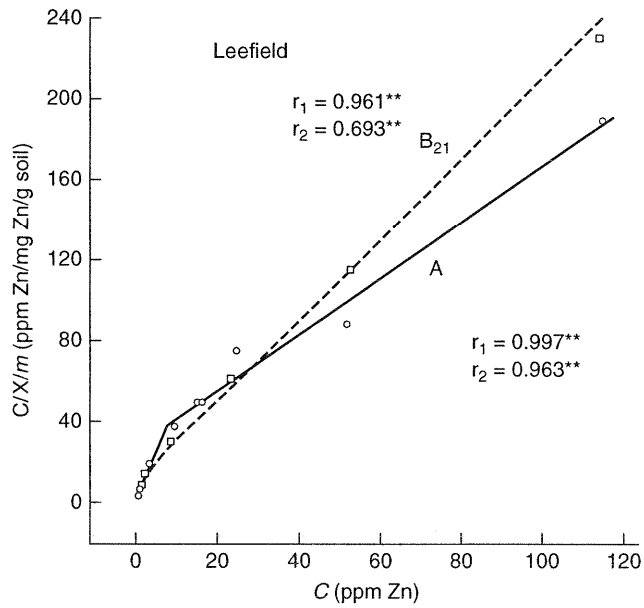

Figure 6.4. Fit of the two surface Langmuir adsorption isotherm equation to zinc adsorption by two soil horizons. (From Shuman, 1975.)

for an adsorption process must be available before any chemical significance can be attributed to isotherm equation parameters. Since use of these equations constitutes a curve-fitting procedure, isotherm equation parameters are valid only for the chemical conditions under which the experiment was conducted. Use of these equations for prediction of metal adsorption behavior under changing conditions of solution pH, solution ionic strength, and solution metal concentration is impossible.

6.2.2. Chemical Surface Complexation Models

Various chemical surface complexation models have been developed to describe potentiometric titration and metal adsorption data at the oxide–mineral solution interface. Surface complexation models provide molecular descriptions of metal adsorption using an equilibrium approach that defines surface species, chemical reactions, mass balances, and charge balances. Thermodynamic properties such as solid-phase activity coefficients and equilibrium constants are calculated mathematically. The major advancement of the chemical surface complexation models is consideration of charge on both the adsorbate metal ion and the adsorbent surface. In addition, these models can provide insight into the stoichiometry and reactivity of adsorbed species. Application of these models to reference oxide minerals has been extensive, but their use in describing ion adsorption by clay minerals, organic materials, and soils has been more limited.

Surface complexation models of the solid–solution interface share at least six common assumptions: (1) surfaces can be described as planes of constant electrical potential with a specific surface site density; (2) equations can be written to describe reactions between solution species and the surface sites; (3) the reactants and products in these equations are at local equilibrium and their relative concentrations can be described using mass law equations; (4) variable charge at the mineral surface is a direct result of chemical reactions at the surface; (5) the effect of surface charge on measured equilibrium constants can be calculated; and (6) the intrinsic (i.e., charge and potential independent) equilibrium constants can then be extracted from experimental measurements (Dzombak and Morel, 1990; Koretsky, 2000).

Four chemical surface complexation models that have been applied to metal and metalloid adsorption by reference minerals or soil systems are described. The first three models (i.e., the constant capacitance model, the diffuse double layer model, and the triple layer model) use the same approach in writing chemical reactions between the bulk solution and the solid surface. Each of these models assumes that all of the sites on a solid surface can be described by average surface site characteristics. If two or more surface site types are used to fit adsorption data with these models, the site types are still generic in nature, with no specific correlation to the solid surface structure. In contrast, the fourth model (i.e., the CD-MUSIC model) distinguishes between different surface site types based on crystal chemical considerations. The first three models differ in their approach and level of detail used to describe the charge and electric potential gradients at the solid–solution interface. The CD-MUSIC model has been implemented with two different descriptions of the electric potential gradient from the solid surface into bulk solution. In all four models, the surface sites are amphoteric surface hydroxyl groups that protonate and deprotonate as a function of pH.

6.2.2.1. Constant Capacitance Model The constant capacitance model of the oxide–solution interface (Schindler et al., 1976; Stumm et al., 1980) contains the following assumptions:

1. All ions, including protons and hydroxyls, adsorb in one surface plane, forming inner-sphere surface complexes.
2. No surface complexes are formed with ions from the background electrolyte.
3. The constant ionic medium reference state determines the activity coefficients of the aqueous species.
4. Surface complexes exist in a chargeless environment in the standard state.
5. The relationship between surface charge, σ, and surface potential, Ψ, is linear and given by

$$\sigma = \frac{CSa}{F}\Psi \tag{6.5}$$

where C is the capacitance (F m^{-2}), S is the surface area (m^2 g^{-1}), a is the particle concentration (g L^{-1}), F is the Faraday constant (C mol_c^{-1}), σ has units of mol_c L^{-1}, and Ψ has units of V.

The protonation and dissociation reactions of the surface functional group are postulated as

$$SOH + H^+ \rightleftharpoons SOH_2^+ \tag{6.6}$$

$$SOH \rightleftharpoons SO^- + H^+ \tag{6.7}$$

where SOH represents the surface functional group and S a metal ion in the oxide mineral that is bound to a reactive surface hydroxyl. In clay or soil systems, the surface functional group can also represent an aluminol or silanol group at the edge of a clay mineral particle. Surface complexation reactions used in the constant capacitance model for metal adsorption include

$$SOH + M^{m+} \rightleftharpoons SOM^{(m-1)} + H^+ \tag{6.8}$$

$$2SOH + M^{m+} \rightleftharpoons (SO)_2M^{(m-2)} + 2H^+ \tag{6.9}$$

where M represents a metal ion, m^+ the charge on the metal ion, Eq. (6.8) monodentate, and Eq. (6.9) bidentate binding of the metal ion with the surface oxygen ligands.

The intrinsic equilibrium constant expressions describing the above reactions are

$$K_+(\text{int}) = \frac{[SOH_2^+]}{[SOH]a_{H^+}} \exp\left(\frac{F\Psi}{RT}\right) \tag{6.10}$$

$$K_-(\text{int}) = \frac{[SO^-]a_{H^+}}{[SOH]} \exp\left(\frac{-F\Psi}{RT}\right) \tag{6.11}$$

$$K_M^1(\text{int}) = \frac{[SOM^{(m-1)}]a_{H^+}}{[SOH]a_{M^{m+}}} \exp\left[\frac{(m-1)F\Psi}{RT}\right] \tag{6.12}$$

$$K_M^2(\text{int}) = \frac{[(SO)_2M^{(m-2)}]a_{H^+}^2}{[SOH]^2a_{M^{m+}}} \exp\left[\frac{(m-2)F\Psi}{RT}\right] \tag{6.13}$$

where R is the molar gas constant (J mol^{-1} K^{-1}), T is the absolute temperature (K), and a represents the activity of an aqueous species. Concentrations (mol L^{-1}), represented by square brackets, are used rather than activities for the surface species because activity coefficients for these species are assumed to be equal to 1. The electrostatic potential terms $\exp(-F\Psi_i/RT)$ have been interpreted as surface activity coefficients that correct for the effect of surface charge on surface complexation (e.g., Dzombak and Morel, 1990) or as work contributions to the overall Gibbs electrochemical potential of reaction (Sverjensky and Sahai, 1996).

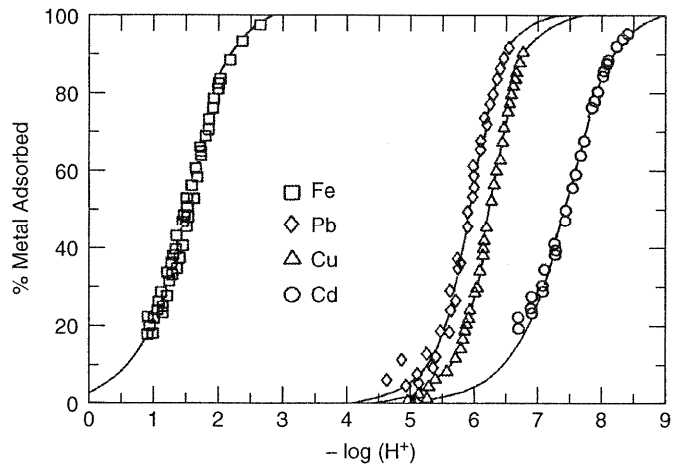

Figure 6.5. Fit of the constant capacitance model to metal adsorption on silica. (From Schindler et al., 1976.)

Recent work by Kulik (2002a,b) and Sverjensky (2003) to define useful standard states for surface species is discussed in Section 6.2.2.5a.

The mass balance for the surface functional group is

$$[\mathrm{SOH}]_T = [\mathrm{SOH}] + [\mathrm{SOH_2}^+] + [\mathrm{SO}^-] + [\mathrm{SOM}^{(m-1)}] + 2[(\mathrm{SO})_2\mathrm{M}^{(m-2)}] \quad (6.14)$$

and the charge balance is

$$\sigma = [\mathrm{SOH_2}^+] - [\mathrm{SO}^-] + (m-1)[\mathrm{SOM}^{(m-1)}] + (m-2)[(\mathrm{SO})_2\mathrm{M}^{(m-2)}] \quad (6.15)$$

This set of equations can be solved by hand or with a computer program using the mathematical approach of Westall (1980). The fit of the constant capacitance model to metal adsorption by silica is shown in Figure 6.5.

6.2.2.2. Diffuse Layer Model The diffuse layer model of the oxide–solution interface (Huang and Stumm, 1973; Dzombak and Morel, 1990) contains the following assumptions:

1. All ions, including protons and hydroxyls, adsorb in one surface plane, forming inner-sphere surface complexes.
2. No surface complexes are formed with ions from the background electrolyte.
3. The infinite dilution reference state is used for aqueous species; a zero surface charge reference state is used for surface species.
4. Two planes of charge represent the interfacial region: the surface plane and a diffuse layer plane that represents the closest distance of approach for the background electrolyte ions.

5. The relationship between surface charge and surface potential is

$$\sigma_d = \frac{Sa}{F}\text{sgn}\Psi_d\left\{2\varepsilon_o DRT\sum_i c_i\left[\exp\left(\frac{-Z_i F\Psi_d}{RT}\right)-1\right]\right\}^{1/2} \tag{6.16}$$

where ε_o is the permittivity of vacuum, D is the dielectric constant of bulk water, $\text{sgn}\Psi_d = 1$ if $\Psi_d > 0$ and $\text{sgn}\Psi_d = -1$ if $\Psi_d < 0$ (where d represents the diffuse plane), and c_i and z_i are the concentration and charge of solution species i, respectively.

In the diffuse layer model the surface reactions include Eqs. (6.6) and (6.7) for protonation and dissociation of the surface functional groups. In the two-site version of the model, surface complexation with metals is considered to occur on at most two types of sites: a small set of high-affinity "strong" sites, S^sOH, and a large set of low-affinity "weak" sites, S^wOH, analogous to Eq. (6.8) (Dzombak and Morel, 1990):

$$S^sOH + M^{m+} \rightleftharpoons S^sOM^{(m-1)} + H^+ \tag{6.17}$$

$$S^wOH + M^{m+} \rightleftharpoons S^wOM^{(m-1)} + H^+ \tag{6.18}$$

Although the diffuse layer model has the capability to consider bidentate metal complexes, such species are not usually considered.

The intrinsic equilibrium constants for the diffuse layer model are similar to those for the constant capacitance model where Ψ is replaced by Ψ_d. Equations (6.10) and (6.11) describe surface protonation and dissociation, respectively. Metal surface complexation is described by two constants similar to that defined in Eq. (6.12) for strong and weak sites:

$$K_M^s(\text{int}) = \frac{[S^sOM^{(m-1)}]a_{H^+}}{[S^sOH]a_{M^{m+}}}\exp\left[\frac{(m-1)F\Psi_d}{RT}\right] \tag{6.19}$$

$$K_M^w(\text{int}) = \frac{[S^wOM^{(m-1)}]a_{H^+}}{[S^wOH]a_{M^{m+}}}\exp\left[\frac{(m-1)F\Psi_d}{RT}\right] \tag{6.20}$$

The mass balances for the surface functional groups S^sOH, S^wOH, and S_T are

$$[S^sOH]_T = [S^sOH] + [S^sOH_2^+] + [S^sO^-] + [S^sOM^{(m-1)}] \tag{6.21}$$

$$[S^wOH]_T = [S^wOH] + [S^wOH_2{}^+] + [S^wO^-] + [S^wOM^{(m-1)}] \tag{6.22}$$

$$S_T = [S^sOH]_T + [S^wOH]_T \tag{6.23}$$

and the charge balance is

$$\sigma_d = [S^sOH_2{}^+] + [S^wOH_2{}^+] - [S^sO^-] - [S^wO^-] + (m-1)[S^sOM^{(m-1)}] + (m-1)[S^wOM^{(m-1)}] \tag{6.24}$$

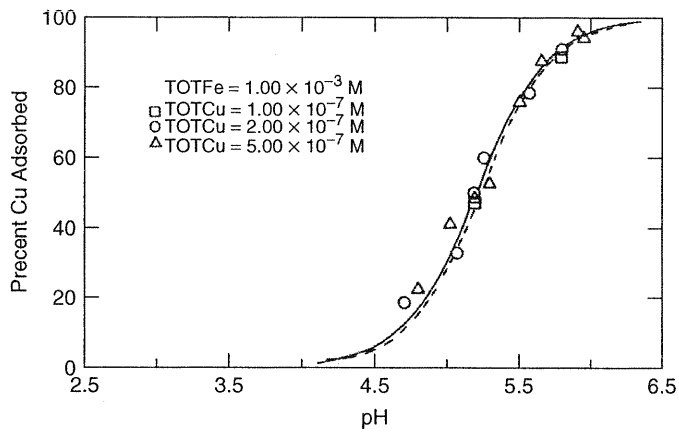

Figure 6.6. Fit of the diffuse layer model to copper adsorption by hydrous ferric oxide. The solid line represents the optimal fit for these data. The dashed line represents the fit corresponding to the best overall estimate of the Cu surface complexation constant obtained from 10 Cu adsorption edges. (From Dzombak and Morel, 1990.)

This set of equations can be approximated with hand calculations or solved using a computer program such as the one described by Dzombak and Morel (1990). An example fit of the diffuse layer model is indicated in Figure 6.6 for copper adsorption to hydrous ferric oxide.

6.2.2.3. Triple Layer Model The triple layer model of the oxide–solution interface (Yates et al., 1974; Davis and Leckie, 1978; Davis et al., 1978; Hayes and Leckie, 1987) contains the following assumptions:

1. Three planes of charge represent the interfacial region: the o-plane, the β-plane, and the d-plane.
2. Protons and hydroxyl ions adsorb in the o-plane.
3. Metals adsorb in either the o-plane or the β-plane.
4. Ions from the background electrolyte adsorb in the β-plane.
5. The diffuse layer plane, the d-plane, represents the closest distance of approach of dissociated charge.
6. Different reference and standard states have been applied to both aqueous and surface species (see below).
7. The relationships between the surface charges, σ_o and σ_d and the surface potentials, Ψ_o, Ψ_β, and Ψ_d are Eq. (6.16) and

$$\sigma_o = \frac{C_1 Sa}{F}(\Psi_o - \Psi_\beta) \tag{6.25}$$

$$\sigma_d = \frac{C_2 Sa}{F}(\Psi_d - \Psi_\beta) \tag{6.26}$$

where C_1 (F m^{-2}), the inner-layer capacitance, relates the charge at the innermost plane of adsorption to the potential drop between the *o*- and the β-planes, and C_2, the outer-layer capacitance, relates the charge at the β-plane to the potential drop between the β-and *d*-planes.

In the triple layer model the surface reactions for protonation and dissociation of the surface functional group are Eqs. (6.6) and (6.7) as written for the constant capacitance model, where Ψ is replaced by Ψ_o. The reactions for adsorption of the background electrolyte in the β-plane are

$$\text{SOH} + \text{C}^+ \rightleftharpoons \text{SO}^- - \text{C}^+ + \text{H}^+ \tag{6.27}$$

$$\text{SOH} + \text{H}^+ + \text{A}^- \rightleftharpoons \text{SOH}_2^+ - \text{A}^- \tag{6.28}$$

where C^+ is the cation and A^- is the anion of the background electrolyte and the dashes indicate that adsorption occurs in the β-plane. Metal ions can adsorb either in the *o*-plane forming surface complexes such as those described by Eqs. (6.8) and (6.9) or in the β-plane by the following surface complexation reactions:

$$\text{SOH} + \text{M}^{m+} \rightleftharpoons \text{SO}^- - \text{M}^{m+} + \text{H}^+ \tag{6.29}$$

$$\text{SOH} + \text{M}^{m+} + \text{H}_2\text{O} \rightleftharpoons \text{SO}^- - \text{MOH}^{(m-1)} + 2\text{H}^+ \tag{6.30}$$

In the triple layer model one of the *o*-plane metal surface complexes is represented as bidentate, Eq. (6.9), while one of the β-plane metal surface complexes is represented as a hydroxy–metal surface species, Eq. (6.30). Davis and Leckie (1978) considered the hydroxy–metal complexation reaction to be more consistent with their experimental data. Often, an additional metal surface complex containing the background electrolyte anion is postulated to form in the β-plane:

$$\text{SOH} + \text{M}^{m+} + \text{A}^- \rightleftharpoons \text{SOHM}^{m+} - \text{A}^- \tag{6.31}$$

The triple layer model has been used with different standard and reference states for both aqueous and surface species (e.g., Davis et al., 1978; Hayes and Leckie, 1987). These differences can result in different "best-fit" surface complexes for the same experimental adsorption data. For example, Hayes and Leckie (1987) expressed both the chemical potentials for aqueous and surface species by the expression

$$\mu_i = \mu_i^o + 2.303RT \log m_i + zF\phi_i \tag{6.32}$$

defining the standard state for both solution and surface species as 1 mol L^{-1} at zero surface charge and no ionic interaction. The reference state for all species was chosen to be infinite dilution relative to the aqueous phase and zero surface charge. The assumption that Eq. (6.32) applies to all aqueous ions is equivalent to abandoning the use of any form of aqueous ion activity coefficients. The outcome

is particularly serious when fitting adsorption data at several ionic strengths. Using this formulation, Hayes and Leckie (1987) found that the surface species $SOCd^+$ and $SOPb^+$ best fit their adsorption data for Cd^{2+} and Pb^{2+} onto goethite from solutions ranging in ionic strength from 0.001 to 1.0 M $NaNO_3$. However, when the activity coefficients for aqueous ions were given by a version of an extended Debye–Hückel equation for 1 : 1 electrolytes (Helgeson et al., 1981), these same data were best fit with surface complexes involving the electrolyte anion $SOHCd^+ - NO_3^-$ and $SOHPb^+ - NO_3^-$ (Criscenti and Sverjensky, 1999). Hayes (1987) found that his pressure-jump kinetic data were also best described by this type of complex.

Some triple layer model intrinsic equilibrium constants for surface complexation in the *o*-plane are Eqs. (6.10) to (6.13) as in the constant capacitance model, where Ψ is replaced by Ψ_o. Possible intrinsic equilibrium constants for surface complexation in the β-plane are

$$K_{C+}(\text{int}) = \frac{[SO^- - C^+]a_{H^+}}{[SOH]a_{C^+}} \exp\left[\frac{F(\Psi_\beta - \Psi_o)}{RT}\right] \tag{6.33}$$

$$K_{A-}(\text{int}) = \frac{[SOH_2^+ - A^-]}{[SOH]a_{H^+}\, a_{A^-}} \exp\left[\frac{F(\Psi_o - \Psi_\beta)}{RT}\right] \tag{6.34}$$

$$K_M^1(\text{int}) = \frac{[SO^- - M^{m+}]a_{H^+}}{[SOH]a_{M^{m+}}} \exp\left[\frac{F(m\Psi_\beta - \Psi_o)}{RT}\right] \tag{6.35}$$

$$K_M^2(\text{int}) = \frac{[SO^- - MOH^{(m-1)}]a_{H^+}^2}{[SOH]a_{M^{m+}}} \exp\left[\frac{F((m-1)\Psi_\beta - \Psi_o)}{RT}\right] \tag{6.36}$$

$$K_M^3(\text{int}) = \frac{[SOHM^{m+} - A^-]}{[SOH]a_{M^{m+}}\, a_{A^-}} \exp\left[\frac{F(m\Psi_o - \Psi_\beta)}{RT}\right] \tag{6.37}$$

The mass balance for the surface functional group when these reactions are considered is

$$\begin{aligned}[SOH]_T = {} & [SOH] + [SOH_2^+] + [SO^-] + [SOM^{(m-1)}] \\ & + 2[(SO)_2M^{(m-2)}] + [SO^- - M^{m+}] + [SO^- - MOH^{(m-1)}] \\ & + [SOHM^{m+} - A^-] + [SO^- - C^+] + [SOH_2^+ - A^-]\end{aligned} \tag{6.38}$$

and the charge balances are

$$\sigma_o + \sigma_\beta + \sigma_d = 0 \tag{6.39}$$

$$\begin{aligned}\sigma_o = {} & [SOH_2^+] + (m-1)[SOM^{(m-1)}] + (m-2)[(SO)_2M^{(m-2)}] \\ & + m[SOHM^{m+} - A^-] + [SOH_2^+ - A^-] \\ & - [SO^-] - [SO^- - M^{m+}] - [SO^- - MOH^{(m-1)}] - [SO^- - C^+]\end{aligned} \tag{6.40}$$

$$\sigma_\beta = m[SO^- - M^{m+}] + (m-1)[SO^- - MOH^{(m-1)}] + [SO^- - C^+] - [SOHM^{m+} - A^-] - [SOH_2^+ - A^-] \quad (6.41)$$

The full set of equations can be solved with a computer program using the mathematical approach outlined by Westall (1980). Caution must be used to ensure that the computer code does not implement the standard and reference states proposed by Hayes and Leckie (1987). A fit of the triple layer model to silver adsorption on amorphous iron oxide is presented in Figure 6.7.

6.2.2.4. Charge Distribution Multisite Complexation Model The charge distribution multisite complexation model (CD-MUSIC) model of the oxide–solution interface (Hiemstra et al., 1989; Hiemstra and van Riemsdijk, 1996) contains the following assumptions:

1. The surface has multiple types of sites.
2. Protons and hydroxyl ions form inner-sphere surface complexes.
3. Two or three electrostatic planes represent the mineral–water interface.
4. Inner-sphere surface complexes have a spatial distribution of charge attributed to two different electrostatic planes, the surface *o*-plane and the intermediate 1-plane.
5. Outer-sphere ion pairs such as those formed with the background electrolyte are located in an outer 2-plane that corresponds to the start of the diffuse double layer.

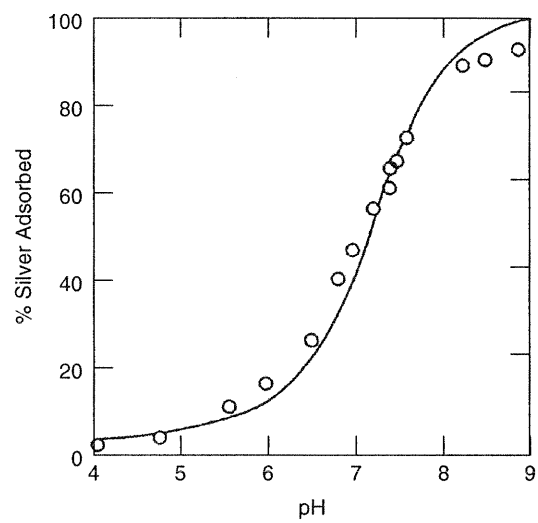

Figure 6.7. Fit of the triple layer model to silver adsorption by amorphous iron oxide. (From Davis and Leckie, 1978.)

6. The charge distribution of the central ion in the surface complex is estimated from the bond valence, ν:

$$\nu = \frac{z}{\mathrm{CN}} \tag{6.42}$$

where z is the charge of the cation and CN is its coordination number. The local formal charge in the surface complex is calculated as the bond valence contribution, s, for each metal and oxygen atom within the oxide structure (Brown and Altermatt, 1985; Hiemstra and van Riemsdijk, 2002; Hiemstra et al., 1996, 2004):

$$s = e^{(R_o - R)/B} \tag{6.43}$$

where R is the metal–oxygen bond length, R_o is an element specific length determined by analysis of the bond valence structure of many crystals, and B is a constant (37 pm). Both R_o and B are empirically determined parameters.

7. The relationships between the surface charges σ_o and σ_1 and the surface potentials Ψ_o, Ψ_1, and Ψ_2 are Eq. (6.16) and

$$\sigma_o = \frac{C_1 Sa}{F}(\Psi_o - \Psi_1) \tag{6.44}$$

$$\sigma_o + \sigma_1 = \frac{C_2 Sa}{F}(\Psi_1 - \Psi_2) \tag{6.45}$$

In the CD-MUSIC model the reactive surface functional group is defined as $S_n\mathrm{OH}^{(n\cdot\nu-1)}$ where n is the number of metal ions in the solid phase coordinated with the reactive surface hydroxyl. The protonation reactions of the surface functional group are

$$\mathrm{S}_n\mathrm{O}^{(n\cdot\nu-2)} + \mathrm{H}^+ \rightleftharpoons \mathrm{S}_n\mathrm{OH}^{(n\cdot\nu-1)} \tag{6.46}$$

$$\mathrm{S}_n\mathrm{OH}^{(n\cdot\nu-1)} + \mathrm{H}^+ \rightleftharpoons \mathrm{S}_n\mathrm{OH}_2^{(n\cdot\nu)} \tag{6.47}$$

Surface complexation with metals produces inner-sphere surface complexes such as

$$\mathrm{S}_n\mathrm{O}^{(n\cdot\nu-2)} + \mathrm{M}^{m+} \rightleftharpoons \mathrm{S}_n\mathrm{OM}^{(n\cdot\nu+m^+-2)} \tag{6.48}$$

$$\mathrm{S}_n\mathrm{OH}^{(n\cdot\nu-1)} + \mathrm{M}^{m+} \rightleftharpoons \mathrm{S}_n\mathrm{OHM}^{(n\cdot\nu+m^+-1)} \tag{6.49}$$

Ion pairing reactions form outer-sphere surface complexes with the background electrolyte:

$$\mathrm{S}_n\mathrm{OH}^{(n\cdot\nu-1)} + \mathrm{C}^+ \rightleftharpoons \mathrm{S}_n\mathrm{OH}^{(n\cdot\nu-1)} - \mathrm{C}^+ \tag{6.50}$$

$$\mathrm{S}_n\mathrm{OH}_2^{(n\cdot\nu)} + \mathrm{A}^- \rightleftharpoons \mathrm{S}_n\mathrm{OH}_2^{(n\cdot\nu)} - \mathrm{A}^- \tag{6.51}$$

The mass balance for the surface functional group when these reactions are considered is:

$$[S_nOH^{(n\cdot v-1)}]_T = [S_nOH^{(n\cdot v-1)}] + [S_nO^{(n\cdot v-2)}] + [S_nOH_2^{(n\cdot v)}] + [S_nOM^{(n\cdot v+m^+-2)}] + [S_nOHM^{(n\cdot v+m^+-1)}] + [S_nOH^{(n\cdot v-1)} - C^+] + [S_nOH_2^{(n\cdot v)} - A^-] \quad (6.52)$$

and the charge balance is (Venema et al., 1996a)

$$\sigma_o + \sigma_1 + \sigma_2 = -\sigma_d \quad (6.53)$$

The charge balance expressions for the surface plane, σ_o, and the intermediate plane, σ_1, are dependent on the charge distribution, as are the intrinsic surface complexation constants. The changes in charges in these planes are given by (Venema et al., 1997)

$$\Delta\sigma_o = \Delta n_H + mf \quad (6.54)$$

$$\Delta\sigma_1 = (1 - f)m \quad (6.55)$$

where Δn_H is the change in the number of protons in the o-plane upon metal adsorption and f is the fraction of the charge of the metal ion assigned to the o-plane. The above set of equations has been solved using the computer program ECOSAT (Keizer and van Riemsdijk, 1995), FITEQL (Tadanier and Eick, 2002), or ORCHESTRA (Meeussen, 2003). The fit of the CD-MUSIC model to cadmium adsorption on goethite is shown in Figure 6.8.

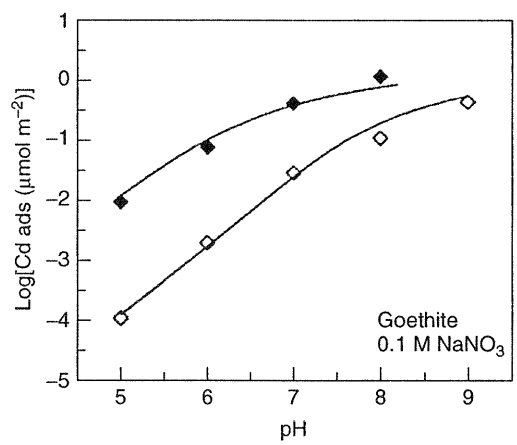

Figure 6.8. Fit of the CD-MUSIC model to cadmium adsorption by goethite. Open symbols represent total dissolved Cd at le-6 mol L^{-1}. Closed symbols represent total dissolved Cd at le-4 mol L^{-1}. (From Venema et al., 1996.)

6.2.2.5. Obtaining Model Parameter Values

a. Standard States for the Activities of Surface Species A variety of standard states for the activities of surface species have been defined explicitly or implied by the way that equilibrium adsorption constants within a surface complexation model framework have been established (Sverjensky, 2003). The choice of standard state affects the equilibrium constant values resulting from fitting adsorption data with a surface complexation model. The standard states that have been used for surface species include the hypothetical 1.0 M standard state (implicitly assumed in Sections 6.2.2.1 to 6.2.2.4), the hypothetical 1.0 m standard state, and the hypothetical 1.0 mol per kilogram of solid standard state. Kulik (2002a,b) examined the standard states used for the Gibbs free energies of individual surface and aqueous species. He focused on the drawbacks to the hypothetical 1.0 M standard state for surface species, such as the built-in dependence on the site density of the solid (Kulik, 2002a). In fact, the molarities of both surface sites and species depend on site densities, surface areas, and solid concentrations (Sverjensky, 2003). These dependencies result in fitted equilibrium constants which cannot be compared directly without correcting for differences in the quantity or properties of the solids used in the experiments.

Sverjensky (2003) proposed new standard states, leading to equilibrium constants independent of the surface area, site density, and the amount of the solid sorbent. These new standard states are dependent only on surface site occupancy and can be used with any surface complexation model. Different standard states are defined for the activities of the sorbent sites and the sorbate species. The theoretical relationships that apply for all adsorption reactions are developed below using Eq. (6.6) as an example reaction.

For the sorbent sites, the standard state refers to unit activity of the sites on a surface where all sorbent sites are SOH, at any temperature and pressure.

$$\overline{\mu}_{\mathrm{SOH}} = \mu^{\#}_{\mathrm{SOH}} + RT \ln \lambda_{\mathrm{SOH}} X_{\mathrm{SOH}} \tag{6.56}$$

where $\overline{\mu}_{\mathrm{SOH}}$ is the electrochemical potential of SOH, $\mu^{\#}_{\mathrm{SOH}}$ is the standard chemical potential for the sorbent sites, λ_{SOH} is the rational activity coefficient for SOH, X_{SOH} is the mole fraction of SOH (the number of moles of SOH per mole of surface sites), and $\lambda_{\mathrm{SOH}} \rightarrow 1$ as $X_{\mathrm{SOH}} \rightarrow 1$. The SOH sites are depicted to follow Raoult's law at high mole fractions. Therefore, the standard state molarity for sorbent sites is not unity. Instead, the standard state molarity depends on the site density, surface area, and amount of the actual sorbent solid:

$$M^{\#}_{\mathrm{SOH}} = \frac{N_s}{N_A} A_s C_s \tag{6.57}$$

where $M^{\#}_{\mathrm{SOH}}$ represents the standard state molarity of sorbent sites SOH, N_s is the surface site density on the sth solid sorbent (sites m^{-2}), A_s is the BET surface area on the sth solid sorbent ($\mathrm{m}^2\ \mathrm{g}^{-1}$), C_s is the amount of the sth sorbent solid ($\mathrm{g\ L}^{-1}$), and N_A is Avogadro's number (6.022×10^{23} sites mol^{-1}).

For the sorbate, the standard state refers to the unit activity of surface species on a completely saturated surface (i.e., all sorbent sites are occupied by sorbate) with zero potential at any temperature and pressure referenced to infinite dilution. The electrochemical potential for SOH_2^+ is

$$\overline{\mu}_{SOH_2^+} = \mu^{\ddagger}_{SOH_2^+} + RT \ln \lambda_{SOH_2^+} X_{SOH_2^+} + F\Psi_{SOH_2^+} \tag{6.58}$$

where $\mu^{\ddagger}_{SOH_2^+}$ is the standard chemical potential for the sorbate species, SOH_2^+ and $\lambda_{SOH_2^+} \rightarrow 1$ as $\Psi_{SOH_2^+} \rightarrow 0$ and $X_{SOH_2^+} \rightarrow 0$. Henry's law is followed at low mole fractions. In the standard state, the sorbate species will have an abundance determined by a *hypothetical* site density, surface area, and amount of solid sorbent. Sverjensky (2003) selected the following standard state values for all solids: $N^{\ddagger} = 10 \times 10^{18}$ sites m^{-2}, $A^{\ddagger} = 10\,m^2\,g^{-1}$, and $C^{\ddagger} = C_s$. Then

$$M^{\ddagger}_{SOH_2^+} = \frac{N^{\ddagger}}{N_A} A^{\ddagger} C^{\ddagger} \tag{6.59}$$

Using these new standard states for the sorbent sites and sorbate species, the equilibrium constant for the surface protonation reaction, Eq. (6.6), is given by

$$K_1^{\theta} = \frac{X_{>SOH_2^+}}{X_{>SOH} a_{H^+}} 10^{F\Psi_o/2.303RT} = \frac{M_{>SOH_2^+}}{M_{>SOH} a_{H^+}} \frac{N_s A_s}{N^{\ddagger} A^{\ddagger}} 10^{F\Psi_o/2.303RT} \tag{6.60}$$

These new equilibrium constants are independent of the properties of the solid and the amount of solid. Without this dependency, equilibrium constants derived from adsorption data on different samples of the same solid, and from adsorption data on different types of solids, can be compared directly.

b. Surface Site Density The total surface site density, N_s, is an important parameter in surface complexation models related to the total number of reactive functional groups. Surface site density values can be obtained using a wide variety of experimental methods, calculated from crystal dimensions, or optimized to fit experimental adsorption data (Davis and Kent, 1990). Experimental methods include potentiometric titration, tritium exchange, maximum ion adsorption, and infrared spectroscopy. Reviews of measured site densities are provided by James and Parks (1982), Davis and Kent (1990), and Koretsky et al. (1998). For one mineral, results from diverse methods can vary up to an order of magnitude with crystallographic calculations yielding the lowest and tritium exchange the highest values (Goldberg, 1991). While goodness-of-fit was found to be insensitive to changes in value of surface site density from 1 to 100 sites nm^{-2} (Hayes et al., 1991), the actual values of the surface complexation constants changed.

To allow the development of self-consistent parameter databases for surface complexation models, Davis and Kent (1990) recommended a surface site density value of 2.31 sites nm^{-2} for natural materials. This value closely approximates

surface site densities for iron and manganese oxides and the edges of clay minerals. It was used successfully to describe boron (Goldberg et al., 2000) and molybdenum (Goldberg et al., 1998, 2002) adsorption on oxides, clay minerals, and soils using the constant capacitance model. An alternative reference site density of 12.05 sites nm^{-2} was proposed by Kulik (2002a) for all mineral–water surfaces because it corresponds roughly to the density of water molecules in a surface monolayer and represents a maximal density of monodentate surface complexes. The standard state proposed by Kulik (2002a) for a surface species is when 1 mol of adsorbate occupies all sites of reference total density on all of the surface of 1 mol of the adsorbent suspended in 1 kg of water–solvent at $P = 1$ bar and at a defined T, in the absence of external fields and at zero surface potential. In contrast, Sverjensky (2003) chose the standard state properties of a surface species to be $N^{\ddagger} = 10$ sites nm^{-2}, $A^{\ddagger} = 10$ m^2 g^{-1}, and $C^{\ddagger} = C_s$ (see Section 6.2.2.5a).

Crystal chemical considerations have been used to calculate the densities of different surface site types for specific minerals (e.g., Jones and Hockey, 1971; Yates, 1975; Hiemstra et al., 1987, 1989; Barron and Torrent, 1996). Koretsky et al. (1998) studied the predominant cleavage or growth faces for a suite of minerals, including goethite, hematite, corundum, kaolinite, albite, anorthite, and quartz. Using calculated bond strengths and charges, "ideal" slices through the crystal structures were defined to be charge-neutral or nearly charge-neutral slices produced with a minimum total strength of bonds severed. Setting the number of broken bonds at the surface equal to the number of reactive surface sites, or considering partial charges of coordinatively unsaturated atoms at the surface, gave the best agreement with available experimentally determined site densities from tritium exchange experiments. In addition, the types of surface hydroxyl groups predicted using this approach were in qualitative agreement with those observed from surface infrared spectroscopy (Koretsky et al., 1998; Koretsky, 2000).

c. Capacitances It has often been stated that capacitances cannot be determined experimentally, and therefore their values must be chosen to optimize model fit to data. This is not strictly correct. Capacitance values for the constant capacitance model can be obtained from the slopes of plots of the conditional protonation-dissociation constants versus surface charge as described by Goldberg (1992). The capacitance value, C_+, obtained from plotting conditional protonation constants is not usually equal to the value, C_-, obtained from plotting conditional dissociation constants. Since computer models for parameter optimization, such as FITEQL (Herbelin and Westall, 1996), require a single value of capacitance, it is usually chosen to optimize model fit to experimental data. This simplification is generally valid since surface complexation constant values are not very sensitive to changes in capacitance value (Goldberg and Sposito, 1984).

In the triple layer model, values of the capacitance, C_1, can be obtained experimentally from the slopes of plots used in linear (Davis et al., 1978), double (James et al., 1978), or electrokinetic (Sprycha, 1984) extrapolations as described

by Goldberg (1992). As for the constant capacitance model, capacitance values, C_{1+}, obtained from extrapolations below the zero point of charge, are not usually equal to the values, C_{1-}, obtained from extrapolations above the zero point of charge. Electrokinetic extrapolation is the only method for determining the value of capacitance C_2 experimentally (Sprycha, 1984). This method assumes that the zeta potential, ζ, is equal to the diffuse layer potential, Ψ_d. Because of these experimental difficulties, capacitance values in the triple layer model have almost universally been treated as adjustable parameters. The capacitance, C_1, is adjusted to optimize fit to experimental data and the value of the capacitance, C_2, is fixed at 0.2 F m^{-2}. Use of this value for C_2 in the triple layer model has been criticized because of its uncertain physical interpretation (Hiemstra and van Riemsdijk, 1991).

Sverjensky (2005) suggested that while the triple layer model fits to surface charge data are not dependent on the value for C_2, the value for C_2 is important for predicting zeta potentials. The small value of 0.2 F m^{-2} implies a rather large distance between the β-and the *d*-planes of the model. Sverjensky (2005) proposed that the separation of these two planes is influenced by the size of the electrolyte cation in the β-plane and assumed that $C_1 = C_2$. Using this assumption, good agreement between predicted and experimental zeta potentials was found for rutile in LiCl and CsCl solutions (Kallay et al., 1994) and for hematite in $NaNO_3$ solutions (Schudel et al., 1997).

Sverjensky (2001) showed that the values for capacitance C_1 obtained for a wide variety of oxides and electrolyte types within the framework of the triple layer model (Sahai and Sverjensky, 1997a) fell into two groups. For rutile, anatase, and magnetite, values of C_1 increased with decreasing crystallographic radius of the electrolyte cation from Cs^+ to Li^+. For quartz, amorphous silica, goethite, hematite, and alumina, values of C_1 increased with decreasing hydrated electrolyte cation radius from Li^+ to Cs^+.

The distance between the *o*- and β-planes was influenced by both the size and state of hydration of the adsorbing electrolyte ions at the β-plane and the presence of water molecules between the planes. These planes do not represent physical distances away from the mineral surface, but rather, planes of constant electric potential. For minerals with high dielectric constants, such as rutile, anatase, and magnetite, the work required for the removal of waters of solvation from cations near the mineral surfaces is negligible (James and Healy, 1972). For these minerals, $1/C_1$ was found to be correlated to the crystallographic radius of the electrolyte cation. On the other hand, for minerals of lower dielectric constant, such as hematite, goethite, alumina, quartz, and amorphous silica, for which the work required to remove waters of solvation near the surface is larger (James and Healy, 1972), C_1 increased in the order of decreasing hydrated radius (Sverjensky, 2001). It should be noted that in this study, regardless of the mineral involved, the electrolyte cations bind into the β-plane of the triple layer model. In this approach, the assignment to the β-plane, a plane of constant electrical potential, does not imply outer-sphere (fully solvated) complexation. Instead, the physical distances to the *o*-plane and the β-plane are substrate dependent.

With his model, Sverjensky (2001) predicted different distances for the adsorption of different electrolyte cations (i.e., $Rb^+ = 3.3$ Å, $Sr^{2+} = 2.9$ Å) at the rutile–water interface that compared well to the distances reported from x-ray standing-wave experiments (Fenter et al., 2000). The model also suggested that trace amounts of metals (e.g., Sr^{2+}, Ca^{2+}) other than the electrolyte cations should form inner-sphere complexes if adsorbed to the β-plane of rutile and similar solids, and form outer-sphere complexes if adsorbed to the β-plane of quartz, goethite, and similar solids. These predictions were consistent with the results of x-ray standing-wave and EXAFS studies (Axe et al., 1998; Fenter et al., 2000; O'Day et al., 2000; Sahai et al., 2000).

In the CD-MUSIC model, C_1 is obtained from titration data and C_2 is chosen to provide a good fit to the salt dependency of specifically adsorbing ions (Hiemstra and van Riemsdijk, 1996). It should be noted that the diffuse layer model does not contain any capacitance parameters.

d. Protonation–Dissociation Constants Values for the intrinsic protonation and dissociation constants can be obtained from the same extrapolation techniques as those used to obtain capacitance values. In the constant capacitance model, the surface complexation constant values are the intercepts obtained by extrapolating alkimetric or acidimetric titration curves to zero net surface charge. Values of intrinsic protonation–dissociation constants obtained for the constant capacitance model using linear extrapolation are compiled in Goldberg (1992).

In the triple layer model, values for the intrinsic protonation and dissociation constants, as well as values for the intrinsic surface complexation constants for the background electrolyte, can be obtained from linear, double, or electrokinetic extrapolations to zero surface charge and zero and infinite electrolyte concentration. Values of intrinsic protonation–dissociation constants and intrinsic surface complexation constants for background electrolytes obtained for the triple layer model using the various extrapolations are compiled in Goldberg (1992). Use of graphical extrapolation methods has been criticized because the triple layer parameter values obtained are not unique (Koopal et al., 1987).

Values for protonation–dissociation constants and surface complexation constants for background electrolytes can also be determined by optimization of potentiometric titration data using a computer program. Computer optimization produces bias-free parameters and provides quality-of-fit criteria and parameter standard deviations. Nonlinear least-squares optimization using the FITEQL program was used to obtain surface complexation constants for the diffuse layer model (Dzombak and Morel, 1990). These authors optimized individual potentiometric titration data sets at each ionic strength and then weighted the individual optimum values to obtain overall best estimates using the following equation:

$$\overline{\log K(\text{int})} = \sum \frac{(1/\sigma_{\log K(\text{int})})_i}{\sum(1/\sigma_{\log K(\text{int})})_i}[\log K(\text{int})]_i \tag{6.61}$$

where $(\sigma_{\log K(\text{int})})_i$ is the standard deviation calculated for log K(int) of the ith data set. Individual protonation-dissociation constants and overall best estimates

for hydrous ferric oxide are presented in Dzombak and Morel (1990). In the CD-MUSIC model, the intrinsic constant for the surface functional group was optimized by trial and error using the ECOSAT computer program (Venema et al., 1996b). In this approach, site densities of the two crystal planes were derived from crystal structure and shape.

Values for protonation–dissociation constants of generic surface sites can also be predicted using solvation and crystal chemical theory (Sverjensky and Sahai, 1996). Using the standard states defined above (Sverjensky, 2003), the values of $\log K_1^{\theta}$ and $\log K_2^{\theta}$ can be calculated from $\log K_{\mathrm{ZPC}}^{\theta}$ and $\log K_n^{\theta}$, which are defined next. At the zero point of charge ($\mathrm{pH_{ZPC}}$), the surface of a metal oxide has a net zero charge and the surface equilibrium can be expressed by

$$\mathrm{SO^- + 2H^+ \rightleftharpoons SOH_2^+} \tag{6.62}$$

and

$$\mathrm{pH_{ZPC}} = 0.5 \log K_{\mathrm{ZPC}}^{\theta} = 0.5\left(|\log K_1^{\theta}| + |\log K_2^{\theta}| \right) \tag{6.63}$$

The overall equation for equilibrium surface protonation is

$$\mathrm{SO^- + SOH_2^+ \rightleftharpoons 2SOH} \tag{6.64}$$

and the equilibrium constant expression is

$$\log K_n^{\theta} = \log \frac{a_{\mathrm{SOH}}^2}{a_{\mathrm{SO^-}}\, a_{\mathrm{SOH_2^+}}} = \log K_2^{\theta} - \log K_1^{\theta} \tag{6.65}$$

Sverjensky and Sahai (1996) proposed that the standard Gibbs free energy of the νth surface protonation reaction ($\Delta G_{r,\nu}^0$) can be broken into three terms according to

$$\Delta G_{r,\nu}^0 = \Delta G_{s,\nu}^0 + \Delta G_{pi,\nu}^0 + \Delta G_{ii,\nu}^0 \tag{6.66}$$

where $\Delta G_{s,\nu}^0$ represents a Born solvation contribution, $\Delta G_{pi,\nu}^0$ an electrostatic interaction term, and $\Delta G_{ii,\nu}^0$ a term intrinsic to the aqueous proton. The Born solvation term is treated by building on earlier studies of metal adsorption (James and Healy, 1972). The proton interaction term is built by summing an attractive interaction between the proton and the surface oxygen with a repulsive interaction between the proton and the underlying metal of the solid sorbent (Yoon et al., 1979).

Predictive equations for the equilibrium surface protonation constants derived using the approach of Sverjensky and Sahai (1996) are

$$\log K_{\mathrm{ZPC}}^{\theta} = \frac{-\Delta\Omega_{r,\mathrm{ZPC}}}{2.303RT}\frac{1}{\varepsilon_s} - B_{\mathrm{ZPC}}\frac{s}{r_{\mathrm{H^+}}} + \log K''_{ii,\mathrm{ZPC}} \tag{6.67}$$

and

$$\log K_n^{\theta} = -B_n \frac{s}{r_{H^+}} + \log K''_{ii,n} \tag{6.68}$$

where ε_s and s/r_{H+} represent the dielectric constant and the Pauling bond strength per angstrom, respectively, for the sth solid. The term involving the dielectric constant of the solid arises from the solvation term in Eq. (6.66), and the terms involving the Pauling bond strength arise from the electrostatic interaction term. The dielectric constant parameter also builds implicitly in a dependence on ionicity of the metal–oxide bond (Sahai, 2002) via the relationships with dielectric constant, polarizability, and ionicity. The $\Delta\Omega_{r,ZPC}$, B_{ZPC}, B_n, $\log K''_{ii,ZPC}$, and $\log K''_{ii,n}$ terms are coefficients obtained by calibrating the equations with experimentally derived equilibrium constants. The symbol $\Delta\Omega_{r,ZPC}$ in Eq. (6.67), represents a Born solvation coefficient for the reaction

$$\Delta\Omega_{r,ZPC} = \Omega_{>SOH_2^+} - \Omega_{>SO^-} = \Omega^{abs}_{>SOH_2^+} - \Omega^{abs}_{>SO^-} \tag{6.69}$$

where the symbols represent the conventional ($\Omega_{>SOH_2^+}$, $\Omega_{>SO^-}$) and absolute Born coefficients ($\Omega^{abs}_{>SOH_2^+}$, $\Omega^{abs}_{>SO^-}$). The relationship between the conventional and absolute Born coefficients for the jth surface species is given by

$$\Omega_j^{abs} = \Omega_j + \Omega^{abs}_{>SOH} \tag{6.70}$$

based on the convention that $\Omega^{abs}_{>SOH} = 0.0$. The absolute solvation coefficient of the jth surface species is calculated using

$$\Omega_j^{abs} = \frac{\eta Z^2 j}{4R_{e,j}} \tag{6.71}$$

where $R_{e,j}$ represents the effective electrostatic radius for the surface species, Z_j represents the charge on the jth species, and $\eta = 166.027$ kcal Å mol^{-1} (Sverjensky, 1993). The effective electrostatic radius of surface species is defined as

$$R_{e,j} = r_{x,j} + \gamma_Z \tag{6.72}$$

where $r_{x,j}$ represents a crystallographic radius and γ_Z represents a constant for cations or anions for a given charge. Sverjensky and Sahai (1996) showed that values for the coefficients $\Delta\Omega_{r,ZPC}$, B_{ZPC}, B_n, $\log K''_{ii,ZPC}$, and $\log K''_{ii,n}$ in Eqs. (6.67) and (6.68) can be found within the framework of the constant capacitance, diffuse layer, or triple layer model by regressing experimentally determined values for $\log K^{\theta}_{ZPC}$ and $\log K_n^{\theta}$. These equations can then be used to determine surface protonation–dissociation constants for other metal oxides given the dielectric constants and the Pauling bond strength per angstrom for the metal–oxygen bonds within these solid phases.

According to Bickmore et al. (2003, 2004), bond relaxation may actually be a key to understanding surface acidity constants. With ab initio methods, Bickmore et al. (2003, 2004) calculated the molecular structures of (hydr)oxide solution monomers and the relaxation of mineral surfaces. Bond-valence methods for the prediction of solution and surface functional group acidity constants were reevaluated based on these calculated structures. It was found that the acidity constants for oxyacids and hexaaquo cations are correlated to the Lewis base strength, S_b, of a conjugate base and metal–oxygen bond ionicity, I, and cannot be treated with the same model. The acidity constants for both –OH and $-OH_2$ surface functional groups, were found to be correlated to S_b and I through the same regression equation as the acidity constants for solution oxyacids:

$$pK_a^{int}(\pm 0.83) = 61.5S_b + 22.5I - 19.2 \tag{6.73}$$

e. Metal Surface Complexation Constants Metal surface complexation constants can be evaluated graphically, although this necessitates the simplifying assumption that $\Psi = 0$. This limitation can be overcome by computer optimization of the constants. Metal surface complexation constants for all models have been obtained using various computer programs, including MICROQL (Westall, 1979), FITEQL (Herbelin and Westall, 1996), HYDRAQL (Papelis et al., 1988), and ECOSAT (Keizer and van Riemsdijk, 1995). All of the models contain different basic assumptions for the solid–solution interface. Therefore, surface complexation constants obtained with one model must never be used in any other model. Model parameter values are interdependent, so that values obtained for the surface complexation constants are dependent on the values chosen for surface site density and capacitances. Scientists must be aware of all input parameter values used when extracting surface complexation constant values from the literature.

In the absence of experimental data, the equilibrium constants for electrolyte cation and anion adsorption for the triple layer model can also be estimated based on free energy correlation type equations using the internally consistent parameter sets developed by Sverjensky and Sahai (1996), Sahai and Sverjensky (1997a,b), and Koretsky et al. (1998) and expanded in more recent papers (Criscenti and Sverjensky, 1999, 2002; Sverjensky, 2005). These parameters can be calculated using the computer program, GEOSURF (Sahai and Sverjensky, 1998). The standard Gibbs free energy for adsorption of the νth electrolyte cation or anion is broken down into three terms, representing a Born solvation contribution, an electrostatic interaction between the adsorbate and the surface, and an energy intrinsic to the aqueous adsorbate. This expression is analogous to Eq. (6.66) for surface protonation. The equilibrium constants for the electrolyte cation and anion can be predicted from expressions similar to Eq. (6.67) for $\log K^{\theta}_{ZPC}$:

$$\log K^{\theta}_{M^+} = \frac{-\Delta\Omega_{r,M^+}}{2.303RT}\frac{1}{(\varepsilon_s)} - B_{M^+}\frac{s}{(r_{M^+})} + \log K''_{ii,M^+} \tag{6.74}$$

$$\log K^{\theta}_{L^+} = \frac{-\Delta\Omega_{r,L^-}}{2.303RT}\frac{1}{(\varepsilon_s)} - B_{L^-}\frac{s}{(r_{L^-})} + \log K''_{ii,L^-} \tag{6.75}$$

where s represents the Pauling bond strength (Sverjensky and Sahai, 1996) and r_{M+} and r_{L-} represent the distances by which the adsorbing ions are repulsed by the underlying cation of the solid and the surface oxygen, respectively (Sverjensky, 2005). Values of r_{M+} are estimated by prediction from crystal structure analysis and a theoretical analysis of capacitances (Sverjensky, 2001), while values for r_{L-} are approximated by adding a characteristic distance for each surface to an effective crystallographic radius for L^-. These values are used in regression calculations to obtain the repulsion coefficients B_{M+} and B_{L-} and the ion-specific $\log K''_{ii,M+}$ and $\log K''_{ii,L-}$. Figure 6.9 illustrates the results of several linear regressions using $\log K^{\theta}_{M+}$ and $\log K^{\theta}_{L-}$ values determined by fitting experimental surface charge data using the triple layer model. Figure 6.9*c* shows the inverse correlation between $\Delta\Omega_{r,M+}$ and the effective electrostatic radius of the ion, $R_{e,j}$. Figure 6.9*d* illustrates that $\log K''_{ii,M+}$ can be correlated to the aqueous-phase equilibrium metal hydrolysis constant, $\log K_{M(OH)}$. Analogous correlations can be made for the monovalent anions (Sverjensky, 2005).

In the diffuse layer model, all intrinsic metal surface complexation constants were optimized with the FITEQL program for both the strong and weak sites using the best estimates of the protonation constant, $\overline{\log K_+(\text{int})} = 7.29$, and the dissociation constant $\overline{\log K_-(\text{int})} = -8.93$ obtained with Eq. (6.61) (Dzombak and Morel, 1990). Thus, individual values of $\log K^{s}_{M_i}(\text{int})$ and $\log K^{w}_{M_i}(\text{int})$ and best estimates of $\overline{\log K^{s}_{M_i}(\text{int})}$ and $\overline{\log K^{w}_{M_i}(\text{int})}$ are unique in that they represent a self-consistent thermodynamic database for metal adsorption on hydrous ferric oxide.

Another standardized database for the diffuse layer model was developed for montmorillonite by Bradbury and Baeyens (2005). Surface complexation constants for strong and weak sites and cation exchange were fit to adsorption data for various metals using constant site densities and protonation–dissociation constants in a nonelectrostatic modeling approach. Linear free energy relationships were developed to predict surface complexation constants for additional metals from their aqueous hydrolysis constants.

Recognizing the utility of a standardized database of surface complexation constants, Kulik (2002a) recommended the normalization of intrinsic constants to a reference site density of 12.05 sites nm^{-2}:

$$\log K_{\text{norm}} = \log K(\text{int}) + \log \frac{N_s}{12.05} \tag{6.76}$$

This calculation allows a comparison of surface complexation constants for a particular mineral obtained with a specific surface complexation model. A set of constants normalized in this manner can be used to provide a self-consistent surface speciation.

The Rossendorf expert system for surface and sorption thermodynamics, RES^{3}T (Brendler et al., 2003, 2004), is a mineral-specific digitized thermodynamic database that contains mineral properties, specific surface areas, ion sorption data, surface complexation reactions, and bibliographic information based

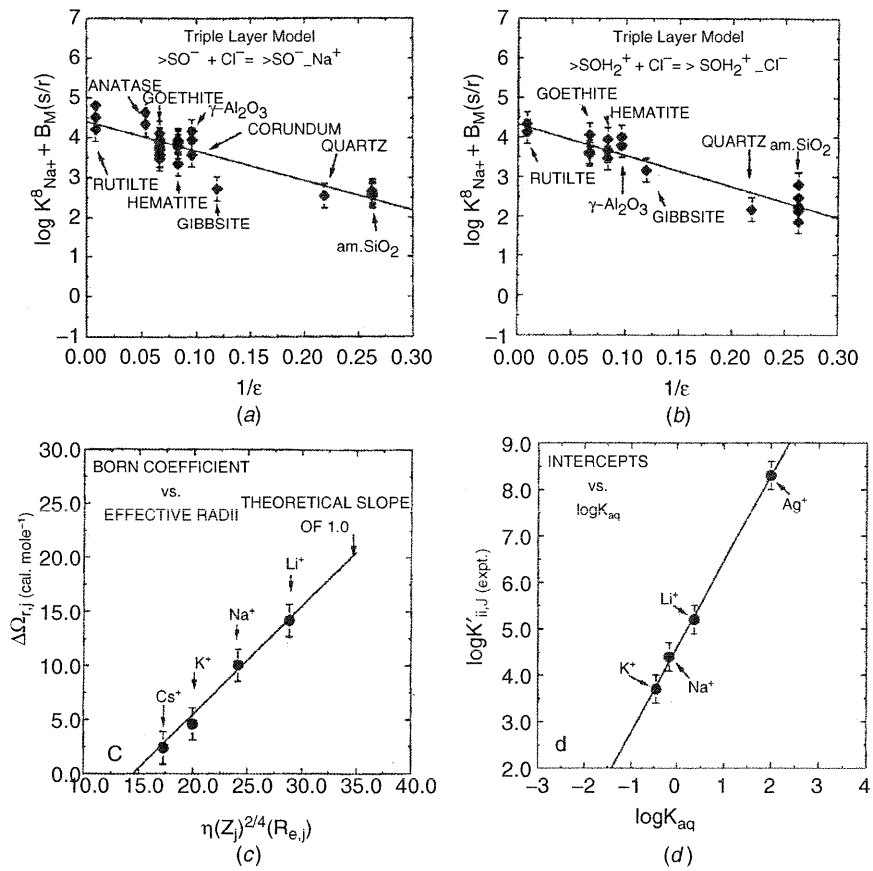

Figure 6.9. (*a*) Values of log $K^{\theta}_{M^+}$ as a function of the dielectric constant $(1/\varepsilon_s)$ and values of the bond strength per Å (s/r_{M^+}); (*b*) values of log $K^{\theta}_{L^-}$ as a function of the dielectric constant $(1/\varepsilon_s)$ and the repulsive term in Å $(2/r_{L^+})$; (*c*) values of $\Delta\Omega_{r,M^+}$ as a function of the effective electrostatic radius $(1/R_{e,j})$ and values of $r_{x,j}$; (*d*) linear free energy correlations for values of $\log K''_{ii,M^+}$ with the aqueous-phase equilibrium association constants $K_{M(OH)^0}$. (From Sverjensky, 2005.)

presently on 1460 literature references. Surface complexation approaches considered include the constant capacitance, diffuse layer, triple layer, and CD-MUSIC models. Data and parameter sets can be exported to other modeling applications. The normalization calculation of Eq. (6.76) is contained as an option in the RES^{3}T database.

The Common Thermodynamic Database Project, CTDP (van der Lee and Lomenech, 2004), is another thermodynamic database that includes sorption equilibrium constants for the constant capacitance model, the diffuse layer model, and

the triple layer model. At present the database includes 330 surface species for nine solids and is formatted in XML, a code independent electronic format.

Criscenti and Sverjensky (1999, 2002) continued to build the internally consistent set of triple layer model equilibrium constants developed by Sverjensky and Sahai (1996) and Sahai and Sverjensky (1997a,b) by reexamining sets of adsorption edge and isotherm data for divalent metal cation adsorption onto oxide surfaces. In contrast to previous investigations, they found that the adsorption of transition and heavy metals on solids such as goethite, γ-Al_2O_3, corundum, and anatase, which have dielectric constants between 10 and 22, was best described by surface complexes of the metal with the electrolyte anion. Metal (M^{2+}) adsorption from $NaNO_3$ solutions is described by

$$SOH + M^{2+} + NO_3^- \rightleftharpoons SOHM^{2+} - NO_3^- \tag{6.77}$$

from $NaClO_4$ solutions by

$$SOH + M^{2+} + ClO_4^- \rightleftharpoons SOHMClO_4^+ \tag{6.78}$$

from NaCl solutions by

$$SOH + M^{2+} + Cl^- \rightleftharpoons SOHMCl^+ \tag{6.79}$$

Adsorption of these same metals onto solids such as quartz and silica, with low dielectric constants between 4 and 5, may be accompanied by the electrolyte anion in $NaClO_4$ solutions, but in $NaNO_3$ and NaCl solutions, metal adsorption occurred as SOM^+ or SOMOH. The large Born solvation free energies on low dielectric constant solids opposed the coadsorption of the electrolyte anion. Using the triple layer model with metal–anion surface complexes, isotherms of metal adsorption over a range of surface coverages could be described with a single-site model, presenting an alternative to the concept that changes in isotherm slope reflect the filling of different types of surface sites (Criscenti and Sverjensky, 2002). Because the equilibrium constants reported by Criscenti and Sverjensky (1999, 2002) preceded the work of Sverjensky (2003) on standard and reference states for mineral–water interfaces, they should be modified according to Eq. (6.60). The choice of surface complexes that best fit the adsorption edge and isotherm curves should not be affected by more recent studies (Sverjensky, 2001, 2003, 2005).

6.2.2.6. Establishing Ion Adsorption Mechanisms and Surface Speciation In using surface complexation models, the user must specify the adsorption mechanisms and types of surface complexes for all adsorbing metal and metalloid ions. To preserve the chemical significance of surface complexation models, adsorption mechanisms should be established from independent experiments. Spectroscopic techniques can be used to provide direct experimental evidence of metal and metalloid adsorption mechanisms. Indirect experimental procedures of establishing adsorption mechanisms include point of zero charge shifts and ionic strength dependence.

a. Spectroscopic Techniques

VIBRATIONAL SPECTROSCOPY Infrared and Raman spectroscopies have proven to be useful techniques for studying the interactions of ions with surfaces. Direct evidence for inner-sphere surface complex formation of metal and metalloid anions has come from vibrational spectroscopic characterization. Both Raman and Fourier transform infrared (FTIR) spectroscopies are capable of examining ion adsorption in wet systems. Chromate (Hsia et al., 1993) and arsenate (Hsia et al., 1994) were found to adsorb specifically on hydrous iron oxide using FTIR spectroscopy. Raman and FTIR spectroscopic studies of arsenic adsorption indicated inner-sphere surface complexes for arsenate and arsenite on amorphous iron oxide, inner-sphere and outer-sphere surface complexes for arsenite on amorphous iron oxide, and outer-sphere surface complexes for arsenite on amorphous aluminum oxide (Goldberg and Johnston, 2001). These surface configurations were used to constrain the surface complexes in application of the constant capacitance and triple layer models (Goldberg and Johnston, 2001).

NUCLEAR MAGNETIC RESONANCE SPECTROSCOPY Nuclear magnetic resonance (NMR) spectroscopy can be applied to aqueous samples and can distinguish between inner- and outer-sphere ion surface complexes. The adsorption behavior of the cations Cs^+ and Na^+ was studied on the surfaces of silica, boehmite, kaolinite, and illite (Kim and Kirkpatrick, 1997). Cesium was adsorbed both as inner-and outer-sphere surface complexes and in the diffuse layer, while Na was adsorbed only as outer-sphere surface complexes and in the diffuse layer. The adsorbed Na ions were fully hydrated, while the Cs ions had direct contact with the surface oxygen atoms.

ELECTRON SPIN RESONANCE SPECTROSCOPY Electron spin resonance (ESR) is a technique that can also be used on aqueous samples and has been used to study the adsorption of copper, manganese, and chromium on aluminum oxides and hydroxides. Copper(II) was found to adsorb specifically on amorphous alumina and microcrystalline gibbsite forming at least one Cu–O–Al bond (McBride, 1982; McBride et al., 1984). Manganese(II) adsorbed on amorphous aluminum hydroxide was present as a hydrated outer-sphere surface complex (Micera et al., 1986). Electron spin resonance combined with electron spin-echo experiments revealed that chromium(III) was adsorbed as an outer-sphere surface complex on hydrous alumina that gradually converted to an inner-sphere surface complex over 14 days of reaction time (Karthein et al., 1991).

X-RAY ABSORPTION SPECTROSCOPY X-ray absorption spectroscopy (XAS) includes x-ray absorption near-edge (XANES) and extended x-ray absorption fine structure (EXAFS) spectroscopy. An advantage of XAS spectroscopy is that adsorption experiments can be carried out in aqueous systems (Fendorf et al., 1994). X-ray absorption spectroscopy has been used to examine the sorption of both cations and anions to oxide and silicate minerals found in soils, with an emphasis on ions that are potential contaminants in the environment.

Cationic contaminants include numerous heavy metals and transition metals and several alkaline earth and alkali metals. The adsorption reactions of Pb^{2+}, Cd^{2+}, Co^{2+}, Hg^{2+}, Cu^{2+}, Zn^{2+}, Ni^{2+}, UO_2^{2+}, Sr^{2+}, Cs^{+}, and NpO_2^{+} onto different oxide, hydroxide, and aluminosilicate minerals have all been investigated using XAS. The nature of the surface complexes formed has been found to be a function of crystal structure, sorbing cation, ligands present in solution, and surface coverage.

X-ray absorption spectroscopy has provided evidence for inner-sphere bidentate surface complexes of Pb^{2+} on Al_2O_3 (Chisholm-Brause et al., 1990a; Bargar et al., 1996, 1997a; Strawn et al., 1998), goethite (Roe et al., 1991; Bargar et al., 1997b), hematite (Bargar et al., 1997b), and amorphous iron oxide (Trivedi et al., 2003). Using grazing-incidence XAFS on single crystals of α-Al_2O_3, Bargar et al. (1996) reported that inner-sphere Pb^{2+} complexes formed preferentially on the (0001) surface, while outer-sphere Pb^{2+} complexes formed on the (11 $\bar{0}$2) surface. On montmorillonite, the type of Pb^{2+} surface complex that formed was a function of ionic strength (Strawn and Sparks, 1999). At low ionic strengths, Pb^{2+} adsorption to montmorillonite was pH independent and XAS suggested that an outer-sphere complex formed. At higher ionic strength, Pb^{2+} adsorption became pH dependent and XAS suggested that inner-sphere complexes formed. Dyer et al. (2003) were able to describe Pb^{2+} adsorption on amorphous iron oxide with the triple layer model using the bidentate mononuclear and monodentate mononuclear surface species observed in the XAS study of Trivedi et al. (2003).

Randall et al. (1999) studied the structure and composition of Cd^{2+} complexes sorbed on several iron oxyhydroxide minerals: goethite, lepidocrocite, akagenite, and schwertmannite using EXAFS. In all cases, adsorbed Cd^{2+} formed inner-sphere complexes over a wide range of solution pH and Cd^{2+} concentration. However, the bonding mechanism differed between minerals and depended on the availability of different types of adsorption sites at the mineral surface. For example, Cd^{2+} sorbed to goethite by the formation of bidentate surface complexes at corner-sharing sites, while Cd^{2+} sorbed to lepidocrocite by the formation of surface complexes at bi-and/or tridentate edge-sharing sites. Manceau et al. (2000) also found Cd^{2+} to form bidentate surface complexes at corner-sharing sites on goethite but mononuclear, fully hydrated surface complexes on lepidocrocite. Venema et al. (1996b) described Cd^{2+} adsorption on goethite with the CD-MUSIC model using the surface species observed in the EXAFS study of Spadini et al. (1994).

Cobalt adsorption onto γ-Al_2O_3 (Chisholm-Brause et al., 1990b), corundum (Towle et al., 1999), and kaolinite (O'Day et al., 1994) has been studied using XAS. For Co^{2+} adsorption onto kaolinite, O'Day et al. (1994) found that at low surface coverages, Co^{2+} sorbed as an inner-sphere bidentate complex. Using grazing-incidence XAFS on single crystals of corundum, Towle et al. (1999) found that Co^{2+} adsorbed in an inner-sphere fashion, forming a tridentate complex on the (0001) surface and a tetradentate complex on the (11 $\bar{0}$2) surface. Katz and Hayes (1995) describe Co^{2+} adsorption by α-Al_2O_3 with the triple layer

model, using the surface species observed by Chisholm-Brause et al. (1990b) using EXAFS spectroscopy.

X-ray absorption spectroscopy has been used to investigate Zn^{2+} adsorption onto ferrihydrite, goethite, a mixture of α-Al_2O_3 and γ-Al_2O_3, and hydrous manganese oxide. Trivedi et al. (2001a,b) concluded that Zn^{2+} adsorbed to both hydrous ferric oxide and hydrous manganese oxide as an outer-sphere complex but formed an inner-sphere complex on goethite. In contrast, Waychunas et al. (2002) found that Zn^{2+} formed inner-sphere tetrahedrally coordinated bidentate surface complexes on ferrihydrite at low surface coverages. Trainor et al. (2000) found that on alumina at low surface coverages, Zn^{2+} also formed inner-sphere, bidentate, tetrahedrally coordinated surface complexes.

Collins et al. (1999a) found that Hg^{2+} sorbed to goethite as an inner-sphere bidentate complex. Cheah et al. (1998) found that Cu^{2+} sorbed to amorphous silica and γ-Al_2O_3 as monomeric and monodentate inner-sphere surface complexes. However, bidentate complexes may also form on γ-Al_2O_3. Using polarized EXAFS, Dähn et al. (2003) determined that Ni^{2+} sorbed to montmorillonite edge sites as an inner-sphere mononuclear surface complex. Inner-sphere surface complexes were observed with XAS for Cr^{3+} adsorption on manganese (Manceau and Charlet, 1992) and iron oxides (Charlet and Manceau, 1992).

Strontium adsorption onto soil minerals is an important retardation mechanism for $^{90}Sr^{2+}$. Chen et al. (1998) investigated the adsorption of Sr^{2+} onto kaolinite, illite, hectorite, and montmorillonite over a range of ionic strengths and from two different electrolyte solutions, $NaNO_3$ and $CaCl_2$. In all cases, the EXAFS spectra suggested Sr^{2+} adsorbed to clay minerals as an outer-sphere mononuclear complex. Sahai et al. (2000) also found that on amorphous silica, goethite, and kaolinite substrates, Sr^{2+} adsorbed as a hydrated surface complex above pH 8.6. On the other hand, Collins et al. (1998) concluded from EXAFS spectra that Sr^{2+} adsorbed as an inner-sphere complex on goethite.

Bostick et al. (2002) studied Cs^{+} adsorption onto vermiculite and montmorillonite with EXAFS and found that Cs^{+} formed both inner-and outer-sphere complexes on both aluminosilicates. The inner-sphere complexes bound to the siloxane groups in the clay structure. Combes et al. (1992) found that NpO_2^{+} adsorbed onto goethite as a mononuclear surface complex. Waite et al. (1994) were successful in describing uranyl adsorption to ferrihydrite with the diffuse layer model using the inner-sphere, mononuclear, bidentate surface complex observed with EXAFS.

X-ray absorption fine structure studies on metal and metalloid anions include arsenate and chromate (Fendorf et al., 1997) on goethite, arsenate (Waychunas et al., 1993) on goethite and hydrous iron oxide, and arsenate on gibbsite (Ladeira et al., 2001). Mixtures of inner-and outer-sphere surface complexes were observed for arsenite on $\gamma - Al_2O_3$ (Arai et al., 2001). Manning and Goldberg (1996) postulated a mixture of bidentate and monodentate surface complexes in modeling arsenate adsorption on goethite consistent with the results of Waychunas et al. (1993). Using EXAFS, Manning et al. (1998) observed a bidentate binuclear

bridging complex for arsenite adsorbed on goethite. This complex was incorporated into the constant capacitance model, and an excellent fit to arsenite adsorption data was obtained. Grossl et al. (1997) used the EXAFS results of Fendorf et al. (1997) to describe arsenate and chromate adsorption on goethite using the constant capacitance model.

X-RAY REFLECTIVITY X-ray reflectivity measurements can provide important information about mineral-water interfaces in situ by accurately determining the position of an adsorbed monolayer relative to the substrate surface. By measuring x-ray reflectivity of calcite, with and without lead, Sturchio et al. (1997) established that the lead ions were located in the surface atomic layer. X-ray reflectivity measurements found rubidium to be specifically adsorbed to the rutile surface at the tetradentate site (Zhang et al., 2004). These authors were able to include this information in the CD-MUSIC model to obtain an accurate description of rubidium adsorption.

b. Point of Zero Charge Shifts The point of zero charge, PZC, of a solid can be obtained directly from electrokinetic measurements and colloidal stability experiments or indirectly from potentiometric titration data. Electrophoretic mobility is a measure of the movement of charged particles in an electric field with zero electrophoretic mobility indicating the condition of zero surface charge. Specific inner-sphere ion adsorption produces shifts in PZC and reversals of electrophoretic mobility with increasing ion concentration (Hunter, 1981). Shifts in PZC have been observed following arsenate (Anderson et al., 1976; Harrison and Berkheiser, 1982; Suarez et al., 1998), arsenite (Pierce and Moore, 1980; Suarez et al., 1998), chromate (Lumsdon et al., 1984), and molybdate (McKenzie, 1983; Goldberg et al., 1996) adsorption on oxide minerals. Consistent with electrophoretic mobility results, an inner-sphere surface complex was postulated to describe molybdate adsorption on oxides and clay minerals with the constant capacitance model (Goldberg et al., 1996). While all adsorption that produces a shift in the PZC is inner-sphere, adsorption that does not shift the PZC may be either inner-sphere or outer-sphere.

c. Ionic Strength Effects Use of ionic strength dependence of adsorption to distinguish between inner-and outer-sphere surface complexes has been advocated for metal ions (Hayes and Leckie, 1987). Ions showing little ionic strength dependence in their adsorption behavior, such as lead, cadmium (Hayes and Leckie, 1987), and arsenate (Hsia et al., 1994; Goldberg and Johnston, 2001), were considered specifically adsorbed as strong inner-sphere surface complexes. Ions showing ionic strength dependence in their adsorption behavior, such as barium (Hayes, 1987) and arsenite (Goldberg and Johnston, 2001), were considered to be weakly bound as outer-sphere surface complexes. McBride (1997) refined this concept, indicating that ions that show decreasing adsorption with increasing ionic strength are adsorbed outer-sphere, whereas ions that show little ionic strength dependence or show increasing adsorption with increasing ionic strength are

adsorbed inner-sphere. Greater adsorption with increasing ionic strength results from the higher activity of counter ions available in solution to compensate the surface charge generated by specific ion adsorption (McBride, 1997). Criscenti and Sverjensky (1999) showed that transition and heavy metals that were thought not to exhibit ionic strength dependence in adsorption behavior, in fact exhibited a dependence that was a function of the solution electrolyte. In $NaNO_3$ solutions, transition and heavy metal ions exhibited no ionic strength dependence in their adsorption behavior; in NaCl solutions, the metals consistently exhibited decreasing adsorption with increasing ionic strength; and in $NaClO_4$ solutions, they exhibited increasing adsorption with increasing ionic strength. In general, for divalent cations, transition and heavy metal adsorption can be described with inner-sphere complexes, and alkaline earth metal adsorption can be described with outer-sphere surface complexes. However, this generalization may not hold up as more experiments are conducted in electrolyte solutions other than $NaNO_3$.

d. Ab initio and Molecular Modeling Ab initio and molecular modeling can be used to investigate the stoichiometries and relative adsorption energies of viable surface complexes and to set bounds on the uncertainties associated with different surface complexation models (Criscenti, 2004). Ab initio and molecular mechanics modeling provides significant information regarding: (1) the stoichiometry of adsorbing species in terms of both the number of bonds an adsorbing species will form with a mineral surface and metal–ligand pairing at the surface, (2) the structure of water at the mineral–water interface and the corresponding structure in the presence of an adsorbing species, and (3) the relative adsorption energies of different possible surface species. Ab initio and molecular modeling simulations can also be valuable tools to examine how various factors, such as: (1) short- and long-range solvation of the ion both in solution and at the mineral surface, (2) the periodic structure of the mineral surface, and (3) the structure and dielectric constant of interfacial water, influence the adsorption process as a whole (Criscenti, 2004).

Quantum mechanics calculations on small clusters of atoms can be used in combination with x-ray absorption fine-structure (EXAFS) data to determine the mechanism of metal binding on oxide surfaces. For example, Collins et al. (1999a) found several geometries for Hg^{2+} adsorption to goethite that were consistent with EXAFS data, but only one that gave calculated Hg–Fe distances consistent with those observed. In this geometry, Hg^{2+} adsorption occurred via two oxygen atoms bound to edge-sharing Fe sites on the (110) surface. This same group of researchers (Collins et al., 1998, 1999b; Randall et al., 1999) combined quantum mechanics calculations and EXAFS data to constrain the geometry of Cd^{2+} and Sr^{2+} surface complexes on goethite and found that these metals were bound to the same type of site as mercury. Peacock and Sherman (2004a) used ab initio calculations in support of their EXAFS data to determine the stoichiometry of adsorbed Cu^{2+} species on several iron oxides. These surface complex stoichiometries were then used to fit experimental Cu^{2+} adsorption data within a diffuse layer or triple layer model framework. The same type of investigation was

conducted for vanadium adsorption to goethite (Peacock and Sherman, 2004b). In this case, fits to sorption edge data using the surface complexes determined from ab initio cluster calculations and EXAFS data were more nebulous.

Classical molecular mechanics approaches have also been used to investigate the adsorption of metal ions to different mineral surfaces from aqueous solution. For example, using a molecular dynamics approach with interatomic force fields, Cygan et al. (1998) examined Cs^+ adsorption onto fully hydroxylated kaolinite surfaces from chloride solutions. Using a different force field approach, Steele et al. (2000) investigated the adsorption of Cu^{2+}, Zn^{2+}, and Cd^{2+} to the (001) muscovite surface. The calculations showed that these metals do not form strong bonds with the smooth basal plane of muscovite. However, upon the introduction of edge-like defects, both Cu^{2+} and Zn^{2+} cations were bound strongly to the defect sites with bond lengths and coordination numbers in agreement with experiment.

A large research effort has been under way to develop a comprehensive picture of the interface between aqueous solution and the (110) surface of rutile (α-TiO_2). This effort has combined molecular-scale and macroscopic approaches, including experimental measurements, quantum mechanics calculations, molecular simulations, and Gouy–Chapman–Stern models (Zhang et al., 2004). Ab initio calculations and molecular dynamics simulations, validated through direct comparison with x-ray standing-wave measurements, were used to predict ion distributions not measured experimentally. Surface oxygen proton affinities computed using the CD-MUSIC model have been improved by the incorporation of ab initio bond lengths and partial charges. All cations considered (Na^+, Rb^+, Ca^{2+}, Sr^{2+}, Zn^{2+}, Y^{3+}, Nd^{3+}) were found to adsorb as inner-sphere species directly to surface oxygen atoms, while the specific binding geometries and reaction stoichiometries were dependent on ionic radius. This investigation illustrated the success of using different types of modeling to investigate adsorption reactions.

6.3. ADVANTAGES OF SURFACE COMPLEXATION MODELS

The major advantage of the surface complexation models over the empirical approaches is that they have the potential to be predictive in nature and applicable to more than one field site. However, this potential has yet to be realized in a general way. Surface complexation models account for the surface charge arising from the charging of the reactive surface functional group and from metal surface complexation reactions. The models define specific surface species, chemical reactions, mass balances, and charge balances. Goodness-of-fit to experimental adsorption data cannot be used as evidence for the presence of any postulated surface complex. Chemical significance is optimized if as many parameters as possible are obtained experimentally. If there is no independent experimental evidence allowing the determination of the exact structure of adsorbed surface complexes, the use of models having chemical simplicity and a small number of adjustable parameters is preferable.

6.4. APPLICATIONS TO NATURAL SYSTEMS AND LIMITATIONS OF SURFACE COMPLEXATION MODELS

6.4.1. Single- or Two-Site Assumption

In most surface complexation models, metal adsorption edge and isotherm data can be described by assuming that the metal adsorbs to one or at most two average sets of reactive surface sites. This is clearly a gross simplification since natural materials are complex multisite mixtures having a variety of surface functional groups. Experimental evidence indicates that even synthetic oxide surfaces contain multiple types of surface sites that may undergo metal adsorption reactions (Rochester and Topham, 1979a,b; Benjamin and Leckie, 1980, 1981). Thus, even surface complexation constants determined in pure mineral systems are most likely average composite values. However, even in the CD-MUSIC model, which is able to account for the many types of surface sites available on individual minerals, metal adsorption is often described with only two dominant site types (Venema et al., 1996b). If, in the presence of two or more competing metal ions, the site heterogeneity of oxide surfaces manifests itself as selective metal adsorption by some fraction of the total adsorption sites, then the resulting surface complexation constants for each metal will exhibit some surface composition dependence being average values based on only a fraction of the surface functional groups. The presence of organic matter also complicates description of soil systems since humic and fulvic materials can act both as adsorbates on oxide surfaces and as adsorbents for metal ions.

6.4.2. Reactive Surface Area

In the application of surface complexation models to clay minerals or to soils dominant in clays, the assumption is often made that metal ion adsorption occurs primarily on the aluminol and silanol groups of clay edges. The effect of the permanent charge sites on the adsorption process may not be considered. This simplification may be inappropriate, particularly for metal and metalloid anions, since repulsive electrostatic forces emanating from clay faces may spill over and affect the adsorption process on clay edges (Secor and Radke, 1985).

Surface area is a relative measurement whose value is dependent on scale and measurement technique. The surface area of various amorphous aluminum oxides was affected by various factors, including aging, drying, heating, reaction in aqueous solution, and concentration of the starting reagents during synthesis (Goldberg et al., 2001). Amorphous aluminum oxides of widely differing initial surface areas measured in the dry state had surface areas of comparable magnitude upon reaction in aqueous solution and subsequent redrying; initially, high surface areas decreased and initially low surface areas increased. These results cast doubt on the use of initial BET surface areas as chemical characterization parameters indicative of mineral reactivity and as input parameters into surface complexation models. It is likely that other amorphous oxides may exhibit similar behavior and that evaluation of these systems, especially ferrihydrite, is necessary.

For goethites, an inverse relationship between surface area and adsorption capacity was attributed to variability in surface site density (Hiemstra and van Riemsdijk, 1996; Villalobos et al., 2003). The higher reactive site density of a lower surface area goethite formed by rapid reagent addition was attributed to a higher surface area percentage of (001) faces as observed with atomic force microscopy (Gaboriaud and Ehrhardt, 2003). The higher surface area goethite formed by slow reagent addition had a significantly smaller percentage of (001) faces.

6.4.3. Component Additivity

One approach for modeling adsorption on complex mineral assemblages such as soils and sediments is *component additivity* (CA). This approach attempts to predict adsorption on a complex mineral assemblage using the results of a surface characterization of the assemblage and experimental data and model parameters obtained for adsorption by pure reference minerals (Davis et al., 1998). The simplest mineral assemblage is a binary mixture. Constant capacitance modeling of adsorption of various cations and anions using the additivity concept was unsuccessful for binary mixtures of $Al(OH)_3/Fe(OH)_3$ (Anderson and Benjamin, 1990a) and $SiO_2/Fe(OH)_3$ (Anderson and Benjamin, 1990b). It was found that Al and Si dissolved and reprecipitated on $Fe(OH)_3$ blocking many of its adsorption sites.

A major advantage of a successful CA approach is that the surface complexation model parameters are transferable from one field site to another. Unfortunately, at present, CA approaches suffer from significant problems (Davis et al., 2004). In the estimation of surface site types and surface area abundances, it is assumed that the relative mineral surface areas can be estimated from bulk weight abundances and that the surface area of minerals in the assemblage is the same as that of reference minerals used in the laboratory. The lack of fundamental data on the effects of competitive adsorption of solutes common in soil solution and groundwater could lead to overestimation of adsorption due to competitive ion effects on adsorption in the natural system. The lack of fundamental data on the effects of solutes common in soil solution and groundwater on surface charge and surface potentials introduces the potentially erroneous assumption that these ions are not potential determining. Some computer optimization programs (eg., FITEQL) require use of the same surface complexation model, capacitance(s), and surface potentials for all component minerals (Davis et al., 2004).

A CA approach described zinc adsorption on aquifer sand material from Cape Cod by assuming that the aluminum and iron phases present in the quartz grain coatings have a surface area and site density similar to those of poorly crystalline materials (Davis et al., 1998). A similar approach provided only a semiquantitative prediction of uranium adsorption on an alluvial aquifer sediment from Naturita, Colorado, depending on the assumptions made about the relative amounts of surface area of quartz, ferrihydrite, and goethite (Davis et al., 2004). In both of these studies, the surface complexation model considered

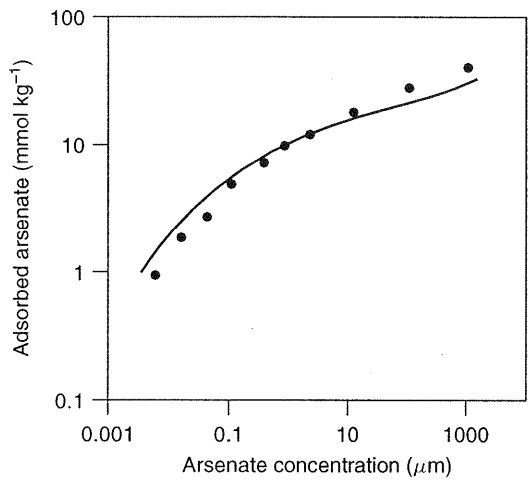

Figure 6.10. Ability of the component additivity approach to describe arsenate adsorption by a soil. (From Gustaffson, 2001.)

was a nonelectrostatic model that did not include electrostatic terms or protonation–dissociation constants. Because of the exclusion of the electrostatic terms, the mass action equations are not expected to provide accurate representations of reaction stoichiometry at the molecular scale (Davis et al., 2004).

Gustaffson (2001) used an electrostatic CA approach with the CD-MUSIC model to describe arsenate adsorption on a spodic B horizon containing allophane and ferrihydrite. He used the arsenate surface complexation constants obtained on gibbsite to represent allophane. The fit of the model was generally very good, although the fit was not quantitative over the entire range of arsenic surface coverages (see Figure 6.10).

An alternative type of component additivity approach is to use different adsorption models for different adsorbents (Weng et al., 2001, 2002). These authors described Cd^{2+}, Zn^{2+}, and Ni^{2+} binding in soils by combining the diffuse layer model for hydrous ferric oxide, the CD-MUSIC model for goethite, the Donnan model for illite, and the nonideal competitive adsorption (NICA) Donnan model (Kinniburgh et al., 1999) for humic acid.

6.4.4. Generalized Composite

In the generalized composite (GC) approach it is assumed that the adsorption behavior of a complex mineral assemblage can be described by surface complexation reactions written with generic surface functional groups that represent average properties of the assemblage as a whole rather than as specific mineral phases (Davis et al., 1998). The GC approach uses the overall surface area value and fits surface complexation constants to the experimental adsorption data. The number of site types and surface complexes are chosen to provide good data

simulation (Davis et al., 1998). Generalized composite approaches successfully described zinc adsorption on Cape Cod (Davis et al., 1998) and uranium adsorption on Naturita (Davis et al., 2004) aquifer sediments. A GC approach developed from laboratory studies using Naturita sediment could predict in situ K_D values for uranium measured in field experiments of the same sample in contact with groundwater of variable chemical conditions (Curtis et al., 2004). The quality of the prediction is shown in Figure 6.11. In the GC approaches described above, the surface complexation model was nonelectrostatic.

Generalized composite approaches have also been used in application of the constant capacitance model to describe molybdenum (Goldberg et al., 1998) and arsenate adsorption by soil (Goldberg and Glaubig, 1988) and sediments (Gao et al., 2006) and the triple layer model to describe calcium and magnesium adsorption by soil (Charlet and Sposito, 1989). In these applications the electrostatic terms and protonation–dissociation reactions were retained.

The predictive capability of the constant capacitance model to describe metal and metalloid adsorption has been tested (Goldberg et al., 2002; 2005). In this approach a general regression model was used to predict surface complexation constants from easily measured soil chemical properties such as surface area, cation exchange capacity, organic carbon content, inorganic carbon content, aluminum oxide content, and iron oxide content. This approach provided a completely independent model evaluation and was able to predict molybdenum (Goldberg et al., 2002) and arsenate (Goldberg et al., 2005) adsorption on numerous diverse soils having a wide range of chemical characteristics. The predictive capability of this approach is shown in Figure 6.12 for both monodentate and bidentate molybdenum surface configurations and in Figure 6.13 for arsenate adsorption by three soil samples.

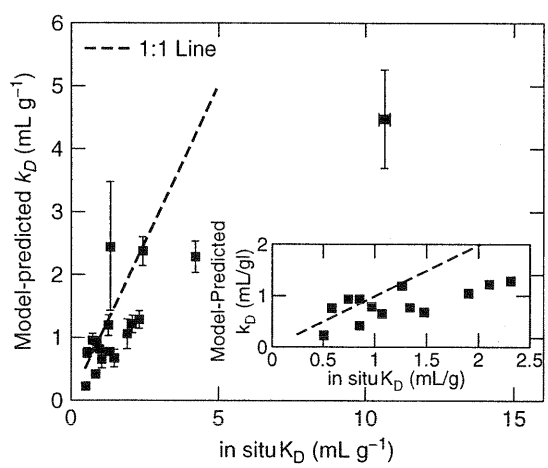

Figure 6.11. Ability of the generalized composite approach to predict K_D values for uranium adsorption on aquifer sediment. (From Curtis et al., 2004.)

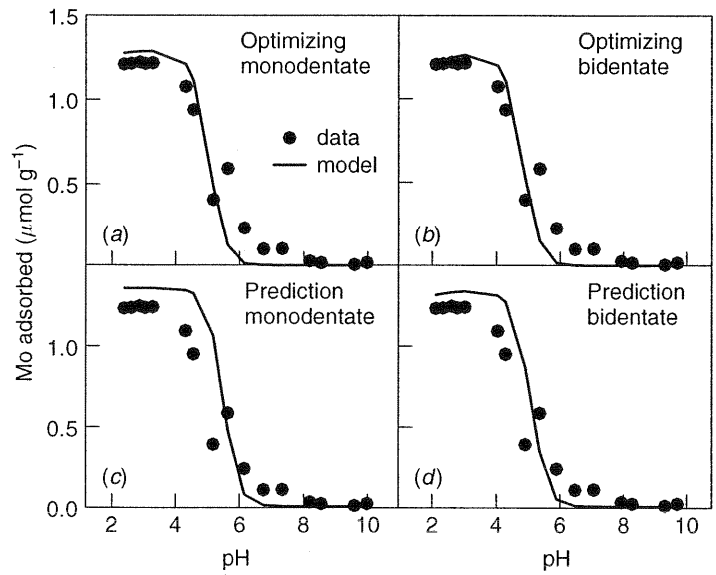

Figure 6.12. Constant capacitance model fits to and predictions of molybdenum adsorption by a soil. (From Goldberg et al., 2002.)

An intercomparison of CA and GC diffuse layer modeling approaches was carried out by 12 teams from eight countries using uranyl adsorption data on the weathered schists from the Koongarra uranium deposit in Australia (Payne et al., 2004). Exclusively predictive CA simulations were unable to provide satisfactory description of the data, and reoptimization of some parameter values was necessary. The GC models provided better simulation of the data but optimized a greater number of model parameters. The ability of either model to describe uranium adsorption on other rock samples from the same field site was unsatisfactory.

6.5. SUMMARY

Various empirical and chemical models of metal adsorption were presented and discussed. Empirical model parameters are only valid for the experimental conditions under which they were determined. Surface complexation models are chemical models that provide a molecular description of metal and metalloid adsorption reactions using an equilibrium approach. Four such models, the constant capacitance model, the diffuse layer model, the triple layer model, and the CD-MUSIC model, were described. Characteristics common to all the models are equilibrium constant expressions, mass and charge balances, and surface activity coefficient electrostatic potential terms. Various conventions for defining the standard state activity coefficients for the surface species have been

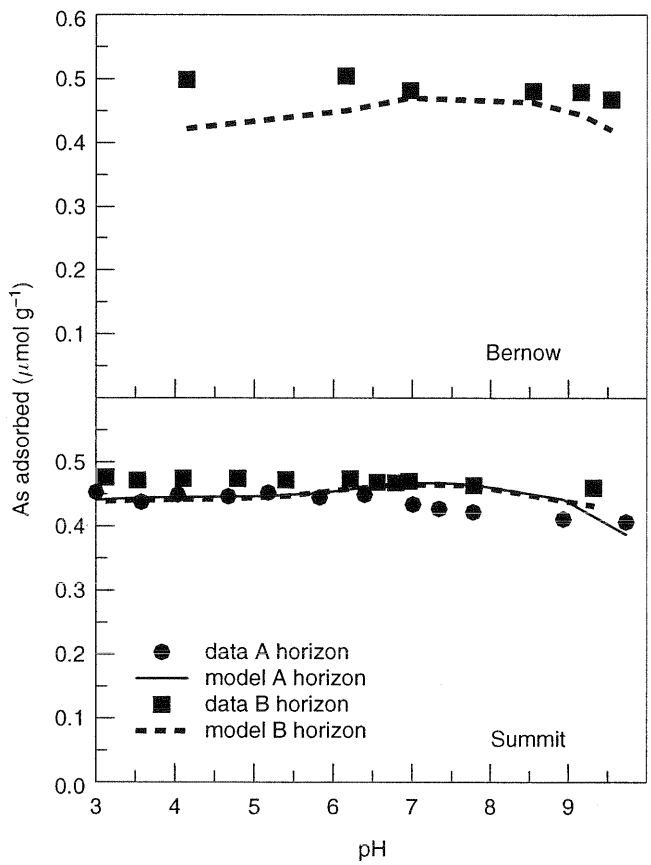

Figure 6.13. Constant capacitance model predictions of arsenate adsorption by three soil samples. (Adapted from Goldberg et al., 2005.)

described. Methods for determining parameter values for surface site density, capacitances, protonation–dissociation constants, and metal surface complexation constants were presented. Experimental methods of establishing metal surface configuration include: vibrational spectroscopy, nuclear magnetic resonance spectroscopy, electron spin resonance spectroscopy, x-ray absorption spectroscopy, and x-ray reflectivity. Metal surface speciation can also be inferred indirectly from point of zero charge shift and ionic strength dependence experiments and ab initio molecular modeling calculations. Applications of the surface complexation models to heterogeneous systems using the component additivity and the generalized composite approaches were described. Continuing research is needed to develop consistent and realistic protocols for describing metal adsorption reactions. The availability of standardized model parameter databases is critical.

Acknowledgments

L. J. Criscenti acknowledges support from the U.S. Department of Energy, Office of Basic Energy Sciences, Division of Chemical Sciences, Geosciences, and Biosciences and the Nuclear Regulatory Commission, Office of Nuclear Regulatory Research. Sandia National Laboratories is a multi-program laboratory operated by the Sandia Corporation, a Lockheed Martin Company for the U.S. Department of Energy's National Nuclear Security Administration under Contract DE-AC04-94AL85000.

REFERENCES

Adamson, A. W. (1976). *Physical Chemistry of Surfaces*, 3rd ed., Wiley, New York.

Anderson, P. R., and Benjamin, M. M. (1990a). Modeling adsorption in aluminum-iron oxide suspensions. *Environ. Sci. Technol.* **24**, 1586–1592.

Anderson, P. R., and Benjamin, M. M. (1990b). Constant capacitance surface complexation model. Adsorption in silica–iron binary oxide suspensions. *Am. Chem. Soc. Symp. Ser.* **416**, 272–281.

Anderson, M. A., Ferguson, J. F., and Gavis, J. (1976). Arsenate adsorption on amorphous aluminum hydroxide. *J. Colloid Interface Sci.* **54**, 391–399.

Arai, Y., Elzinga, E. J., and Sparks, D. L. (2001). X-ray absorption spectroscopic investigation of arsenite and arsenate at the aluminum oxide–water interface. *J. Colloid Interface Sci.* **235**, 80-88.

Axe, L., Bunker, G. B., Anderson, P. R., and Tyson, T. A. (1998). An XAFS analysis of strontium at the hydrous ferric oxide surface. *J. Colloid Interface Sci.* **199**, 44–52.

Bargar, J. R., Towle, S. N., Brown, G. E., and Parks, G. A. (1996). Outer-sphere Pb(II) adsorbed at specific surface sites on single crystal α-alumina. *Geochim. Cosmochim. Acta* **60**, 3541–3547.

Bargar, J. R., Brown, G. E., and Parks, G. A. (1997a). Surface complexation of Pb(II) at oxide–water interfaces. 1. XAFS and bond-valence determination of mononuclear and polynuclear Pb(II) sorption products on aluminum oxides. *Geochim. Cosmochim. Acta* **61**, 2617–2637.

Bargar, J. R., Brown, G. E., and Parks, G. A. (1997b). Surface complexation of Pb(II) at oxide–water interfaces. 2. XAFS and bond-valence determination of mononuclear Pb(II) sorption products and surface functional groups on iron oxides. *Geochim. Cosmochim. Acta* **61**, 2639–2652.

Barron, V., and Torrent, J. (1996). Surface hydroxyl configurations of various crystal faces of hematite and goethite. *J. Colloid Interface Sci.* **177**, 407–410.

Benjamin, M. M., and Leckie, J. O. (1980). Adsorption of metals at oxide interfaces: effects of the concentrations of adsorbate and competing metals. In *Contaminants and Sediments*, ed. Baker, R. A., Vol. 2, Ann Arbor Science, Ann Arbor, MI, 305–322.

Benjamin, M. M., and Leckie, J. O. (1981). Multiple-site adsorption of Cd, Cu, Zn, and Pb on amorphous iron oxyhydroxide. *J. Colloid Interface Sci.* **79**, 209–221.

Bickmore, B. R., Rosso, K. M., Nagy, K. L., Cygan, R. T., and Tadanier, C. J. (2003). Ab initio determination of edge surface structures for dioctahedral 2 : 1 phyllosilicates: implications for acid–base reactivity. *Clays Clay Miner.* **51**, 359–371.

Bickmore, B. R., Tadanier, C. J., Rosso, K. M., Monn, W. D., and Eggett, D. L. (2004). Bond-valence methods for pK_a prediction: critical reanalysis and a new approach. *Geochim. Cosmochim. Acta* **68**, 2025–2042.

Bostick, B. C., Vairavamurthy, M. A., Karthikeyan, K. G., and Chorover, J. (2002). Cesium adsorption on clay minerals: an EXAFS spectroscopic investigation. *Environ. Sci. Technol.* **36**, 2670–2676.

Bradbury, M. H., and Baeyens, B. (2005). Modelling the sorption of Mn(II), Co(II), Ni(II), Zn(II), Cd(II), Eu(III), Am(III), Sn(IV), Th(IV), Np(V), and U(VI) on montmorillonite: linear free energy relationships and estimates of surface binding constants for some selected heavy metals and actinides. *Geochim. Cosmochim. Acta* **69**, 875–892.

Brendler, V., Vahle, A., Arnold, T., Bernhard, G., and Fanghänel, T. (2003). RES^{3}T–Rossendorf expert system for surface and sorption thermodynamics. *J. Contam. Hydrol.* **61**, 281–291.

Brendler, V., Richter, A., Nebelung, C., and Vahle, A. (2004). *Development of a Mineral-Specific Sorption Database for Surface Complexation Modeling.* Part I, *Final Report.* Part II, *Manual*, Project PtWt+E 02E9471, FZ Rossendorf, Dresden, Germany.

Brown, I. D., and Altermatt, D. (1985). Bond-valence parameters obtained from a systematic analysis of the inorganic crystal structure database. *Acta Crystallogr. B* **41**, 244–247.

Cavallaro, N., and McBride, M. B. (1978). Copper and cadmium adsorption characteristics of selected acid and calcareous soils. *Soil Sci. Soc. Am. J.* **42**, 550–556.

Charlet, L., and Manceau, A. A. (1992). X-ray absorption spectroscopic study of the sorption of Cr(III) at the oxide-water interface. II. Adsorption, coprecipitation, and surface precipitation of hydrous ferric oxide. *J. Colloid Interface Sci.* **148**, 443–458.

Charlet, L., and Sposito, G. (1989). Bivalent ion adsorption by an oxisol. *Soil Sci. Soc. Am. J.* **53**, 691–695.

Cheah, S. F., Brown, G. E., and Parks, G. A. (1998). XAFS spectroscopy study of Cu(II) sorption on amorphous SiO_2 and γ-Al_2O_3: effect of substrate and time on sorption complexes. *J. Colloid Interface Sci.* **208**, 110–128.

Chen, C.-C., Papelis, C., and Hayes, K. F. (1998). Extended x-ray absorption fine structure (EXAFS) analysis of aqueous Sr^{II} ion sorption at clay–water interfaces. In *Adsorption of Metals by Geomedia: Variables, Mechanisms, and Model Applications, Proc. American Chemical Society Symposium* ed. Jenne, E. A., Academic Press, San Diego, CA, 333–348.

Chisholm-Brause, C. J., Hayes, K. F., Roe, A. L., Brown, G. E., Parks, G. A., and Leckie, J. O. (1990a). Spectroscopic investigation of Pb(II) complexes at the γ-Al_2O_3/water interface. *Geochim. Cosmochim. Acta* **54**, 1897–1909.

Chisholm-Brause, C. J., O'Day, P. A., Brown, G. E., and Parks, G. A. (1990b). Evidence for multinuclear metal-ion complexes at solid/water interfaces from x-ray absorption spectroscopy. *Nature* **348**, 528–531.

Collins, C. R., Sherman, D. M., and Ragnarsdóttir, K. V. (1998). The adsorption mechanism of Sr^{2+} on the surface of goethite. *Radiochim. Acta* **81**, 201–206.

Collins, C. R., Sherman, D. M., and Ragnarsdóttir, K. V. (1999a). Surface complexation of Hg^{2+} on goethite: mechanism from EXAFS spectroscopy and density functional calculations. *J. Colloid Interface Sci.* **219**, 345–350.

Collins, C. R., Ragnarsdóttir, K. V., and Sherman, D. M. (1999b). Effect of inorganic and organic ligands on the mechanism of cadmium sorption to goethite. *Geochim. Cosmochim. Acta* **63**, 2989–3002.

Combes, J. M., Chisholm-Brause, C. J., Brown, G. E., Parks, G. A., Conradson, S. D., Eller, I. R., Triay, P. G., Hobart, D. E., and Meijer, A. (1992). EXAFS spectroscopic study of neptunium(V) sorption at the α-FeOOH/water interface. *Environ. Sci. Technol.* **26**, 376–382.

Criscenti, L. J. (2004). Adsorption processes: At what spatial scale do we need to understand them? *Proc. 11th International Symposium on Water–Rock Interaction*, WRI-11, Saratoga Springs, NY, June 27–July 2, 2004, ed. Wanty, R. B., and Seal, R. R., A.A. Balkema, New York, 909–916.

Criscenti, L. J., and Sverjensky, D. A. (1999). The role of electrolyte anions (ClO_4^-, NO_3^-, Cl^-) in divalent metal (M^{2+}) adsorption on oxide and hydroxide surfaces in salt solutions. *Am. J. Sci.* **299**, 828–899.

Criscenti, L. J., and Sverjensky, D. A. (2002). A single-site model for divalent transition and heavy metal adsorption over a range of metal concentrations. *J. Colloid Interface Sci.* **253**, 329–352.

Curtis G. P., Fox, P., Kohler, M., and Davis, J. A. (2004). Comparison of in situ uranium K_D values with a laboratory determined surface complexation model. *Appl. Geochem.* **19**, 1643–1653.

Cygan, R. T., Nagy, K. L., and Brady, P. V. (1998). Molecular models of cesium sorption on kaolinite. In *Adsorption of Metals by Geomedia: Variables, Mechanisms, and Model Applications*, ed. Jenne, E. A., Academic Press, San Diego, CA, 383–399.

Dähn, R., Scheidegger, A. M., Manceau, A., Schlegel, M. L., Baeyens, B., Bradbury, M. H., and Chateigner, D. (2003). Structural evidence for the sorption of Ni(II) atoms on the edges of montmorillonite clay minerals: a polarized x-ray absorption fine structure study. *Geochim. Cosmochim. Acta* **67**, 1–15.

Davis, J. A., and Kent, D. B. (1990). Surface complexation modeling in aqueous geochemistry. *Rev. Miner.* **23**, 177–260.

Davis, J. A., and Leckie, J. O. (1978). Surface ionization and complexation at the oxide/water interface. II. Surface properties of amorphous iron oxyhydroxide and adsorption of metal ions. *J. Colloid Interface Sci.* **67**, 90–107.

Davis, J. A., James, R. O., and Leckie, J. O. (1978). Surface ionization and complexation at the oxide/water interface. I. Computation of electrical double layer properties in simple electrolytes. *J. Colloid Interface Sci.* **63**, 480–499.

Davis, J. A., Coston, J. A., Kent, D. B., and Fuller, C. C. (1998). Application of the surface complexation concept to complex mineral assemblages. *Environ. Sci. Technol.* **32**, 2820–2828.

Davis, J. A., Meece, D. E., Kohler, M., and Curtis, G. P. (2004). Approaches to surface complexation modeling of uranium(VI) adsorption on aquifer sediments. *Geochim. Cosmochim. Acta* **68**, 3621–3641.

Dyer, J. A., Trivedi, P., Scrivner, N. C., and Sparks, D. L. (2003). Lead sorption onto ferrihydrite. 2. Surface complexation modeling. *Environ. Sci. Technol.* **37**, 915–922.

Dzombak, D. A., and Morel, F. M. M. (1990). *Surface Complexation Modeling. Hydrous Ferric Oxide*, Wiley, New York.

Fendorf, S. E., Sparks, D. L., Lamble, G. M., and Kelley, M. J. (1994). Applications of x-ray absorption fine-structure spectroscopy to soils. *Soil Sci. Soc. Am. J.* **58**, 1583–1595.

Fendorf, S. E., Eick, M. J., Grossl, P., and Sparks, D. L. (1997). Arsenate and chromate retention mechanisms on goethite. I. Surface structure. *Environ. Sci. Technol.* **31**, 315–320.

Fenter, P., Cheng, L., Rihs, S., Machesky, M. L., Bedzyk, M. J., and Sturchio, N. C. (2000). Elcctrical double-layer structure at the rutile–water interface as observed in situ with small-period x-ray standing waves. *J. Colloid Interface Sci.* **225**, 154–165.

Gaboriaud, F., and Ehrhardt, J.-J. (2003). Effects of different crystal faces on the surface charge of colloidal goethite (α-FeOOH) particles: an experimental and modeling study. *Geochim. Cosmochim. Acta* **67**, 967–983.

Gao, S., Goldberg, S., Herbel, M. J., Chalmers, A. T., Fujii, R., and Tanji, K. K. (2006). Sorption processes affecting arsenic solubility in oxidized surface sediments from Tulare Lake. *Chem. Geol.* **228**, 33–43.

Goldberg, S. (1991). Sensitivity of surface complexation modeling to the site density parameter. *J. Colloid Interface Sci.* **45**, 1–9.

Goldberg, S. (1992). Use of surface complexation models in soil chemical systems. *Adv. Agron.* **47**, 233–329.

Goldberg, S., and Glaubig, R. A. (1988). Anion sorption on a calcareous, montmorillonitic soil–arsenic. *Soil Sci. Soc. Am. J.* **52**, 1297–1300.

Goldberg, S., and Johnston, C. T. (2001). Mechanisms of arsenic adsorption on amorphous oxides evaluated using macroscopic measurements, vibrational spectroscopy, and surface complexation modeling. *J. Colloid Interface Sci.* **234**, 204–216.

Goldberg, S., and Sposito, G. (1984). A chemical model of phosphate adsorption by soils. I. Reference oxide minerals. *Soil Sci. Soc. Am. J.* **48**, 772–778.

Goldberg, S., Forster, H. S., and Godfrey, C. L. (1996). Molybdenum adsorption on oxides, clay minerals, and soils. *Soil Sci. Soc. Am. J.* **60**, 425–432.

Goldberg, S., Su, C., and Forster, H. S. (1998). Sorption of molybdenum on oxides, clay minerals, and soils: mechanisms and models. In *Adsorption of Metals by Geomedia: Variables, Mechanisms, and Model Applications,* ed. Jenne, E. A., *Proc. American Chemical Society Symposium*, Academic Press, San Diego, CA, 401–426.

Goldberg, S., Lesch, S. M., and Suarez, D. L. (2000). Predicting boron adsorption by soils using soil chemical parameters in the constant capacitance model. *Soil Sci. Soc. Am. J.* **64**, 1356–1363.

Goldberg, S., Lebron, I., Suarez, D. L., and Hinedi, Z. R. (2001). Surface characterization of amorphous aluminum oxides. *Soil Sci. Soc. Am. J.* **65**, 78–86.

Goldberg, S., Lesch, S. M., and Suarez, D. L. (2002). Predicting molybdenum adsorption by soils using soil chemical parameters in the constant capacitance model. *Soil Sci. Soc. Am. J.* **66**, 1836–1842.

Goldberg, S., Lesch, S. M., Suarez, D. L., and Basta, N. T. (2005). Predicting arsenate adsorption by soils using soil chemical parameters in the constant capacitance model. *Soil Sci. Soc. Am. J.* **69**, 1389–1398.

Grossl, P., Eick, M. J., Sparks, D. L., Goldberg, S., and Ainsworth, C. C. (1997). Arsenate and chromate retention mechanisms on goethite. II. Kinetic evaluation using a pressure-jump relaxation technique. *Environ. Sci. Technol.* **31**, 321–326.

Gustafsson, J. P. (2001). Modelling competitive anion adsorption on oxide minerals and an allophane-containing soil. *Eur. J. Soil Sci.* **52**, 639–653.

Harrison, J. B., and Berkheiser, V. E. (1982). Anion interactions with freshly prepared hydrous iron oxides. *Clays Clay Miner.* **30**, 97–102.

Hayes, K. F. (1987). Equilibrium, spectroscopic, and kinetic studies of ion adsorption at the oxide/aqueous interface. Ph.D. dissertation, Stanford University, Stanford, CA.

Hayes, K. F., and Leckie, J. O. (1987). Modeling ionic strength effects on cation adsorption at hydrous oxide/solution interfaces. *J. Colloid Interface Sci.* **115**, 564–572.

Hayes, K. F., Redden, G., Ela, W., and Leckie, J. O. (1991). Surface complexation models: an evaluation of model parameter estimation using FITEQL and oxide mineral titration data. *J. Colloid Interface Sci.* **142**, 448–469.

Helgeson, H. C., Kirkham, D. H., and Flowers, G. C. (1981). Theoretical prediction of the thermodynamic behavior of aqueous electrolytes at high pressures and temperatures. IV. Calculation of activity coefficients, osmotic coefficients, and apparent molal and standard and relative partial molal properties to 600°C and 5 KB. *Am. J. Sci.* **281**, 1249–1516.

Herbelin, A. L., and Westall, J. C. (1996). *FITEQL: A Computer Program for Determination of Chemical Equilibrium Constants from Experimental Data,* Rep. 96-01, Version 3.2, Department of Chemistry, Oregon State University, Corvallis, OR.

Hiemstra, T., and van Riemsdijk, W. H. (1991). Physical chemical interpretation of primary charging behavior of metal (hydr)oxides. *Colloids Surf.* **59**, 7–25.

Hiemstra, T., and van Riemsdijk, W. H. (1996). A surface structural approach to ion adsorption: the charge distribution (CD) model. *J. Colloid Interface Sci.* **179**, 488–508.

Hiemstra, T., and van Riemsdijk, W. H. (2002). On the relationship between surface structure and ion complexation of oxide–solution interfaces. In *Encyclopedia of Surface and Colloid Science*, ed. Hubbard, A. T., Marcel Dekker, New York, 3773–3799.

Hiemstra, T., van Riemsdijk, W. H., and Bruggenwert, M. G. M. (1987). Proton adsorption mechanism at the gibbsite and aluminum oxide solid/solution interface. *Neth. J. Agric. Sci.* **35**, 281–293.

Hiemstra, T., van Riemsdijk, W. H., and Bolt, G. H. (1989). Multisite proton adsorption modeling at the solid/solution interface of (hydr)oxides: a new approach. I. Model description and evaluation of intrinsic reaction constants. *J. Colloid Interface Sci.* **133**, 91–104.

Hiemstra, T., Rahnemaie, R., and van Riemsdijk, W. H. (2004). Surface complexation of carbonate on goethite: IR spectroscopy, structure and charge distribution. *J. Colloid Interface Sci.* **278**, 282–290.

Hsia, T. H., Lo, S. L., Lin, C. F., and Lee, D. Y. (1993). Chemical and spectroscopic evidence for specific adsorption of chromate on hydrous iron oxide. *Chemosphere* **26**, 1897–1904.

Hsia, T. H., Lo, S. L., Lin, C. F., and Lee, D. Y. (1994). Characterization of arsenate adsorption on hydrous iron oxide using chemical and physical methods. *Colloids Surf. A: Physicochem. Eng. Asp.* **85**, 1–7.

Huang, C. P., and Stumm, W. (1973). Specific adsorption of cations in hydrous γ-Al_2O_3. *J. Colloid Interface Sci.* **43**, 409–420.

Hunter, R. J. (1981). *Zeta Potential in Colloid Science. Principles and Applications,* Academic Press, London.

James, R. O., and Healy, T. W. (1972). Adsorption of hydrolyzable metal ions at the oxide–water interface. III. A thermodynamic model of adsorption. *J. Colloid Interface Sci.* **40**, 65–81.

James R. O., and Parks, G. A. (1982). Characterization of aqueous colloids by their electrical double-layer and intrinsic surface chemical properties. *Surf. Colloid Sci.* **12**, 119–216.

James, R. O., Davis, J. A., and Leckie, J. O. (1978). Computer simulation of the conductometric and potentiometric titrations of the surface groups on ionizable latexes. *J. Colloid Interface Sci.* **65**, 331–343.

Jones, P., and Hockey, J. A. (1971). Infra-red studies of rutile surfaces. 2. Hydroxylation, hydration and structure of rutile surfaces. *Trans. Faraday Soc.* **67**, 2679–2685.

Kallay, N., Colic, M., Fuerstenau, D. W., Jang, H. M., and Matijevic, E. (1994). Lyotropic effect in surface charge, electrokinetics, and coagulation of a rutile dispersion. *Colloid Polym. Sci.* **272**, 554–561.

Karthein, R., Motschi, H., Schweiger, A., Ibric, S., Sulzberger, B., and Stumm, W. (1991). Interactions of chromium(III) complexes with hydrous δ-Al_2O_3: rearrangements in the coordination sphere studied by electron spin resonance and electron spin-echo spectroscopies. *Inorg. Chem.* **30**, 1606–1611.

Katz, L. E., and Hayes, K. F. (1995). Surface complexation modeling. I. Strategy for modeling monomer complex formation at moderate surface coverage. *J. Colloid Interface Sci.* **170**, 477–490.

Keizer, M. G., and van Riemsdijk, W. H. (1995). *ECOSAT: A Computer Program for the Calculation of Speciation and Transport in Soil–Water Systems,* Tech. Rep., Department of Soil Science and Plant Nutrition, Wageningen Agricultural University, Wageningen, The Netherlands.

Kim, Y., and Kirkpatrick, R. J. (1997). ^{23}Na and ^{133}Cs NMR study of cation adsorption on mineral surfaces: local environments, dynamics, and effects of mixed cations. *Geochim. Cosmochim. Acta* **61**, 5199–5208.

Kinniburgh, D. G. (1985). *ISOTHERM. A Computer Program for Analyzing Adsorption Data*, Rep. WD/ST/85/02, Version 2.2, British Geological Survey, Wallingford, Berkshire, England.

Kinniburgh, D. G., van Riemsdijk, W. H., Koopal, L. K., Borkovec, M., Benedetti, M. F., and Avena, M. J. (1999). Ion binding to natural organic matter: competition, heterogeneity, stoichiometry and thermodynamic consistency. *Colloids Surf. A: Physicochem. Eng. Asp.* **151**, 147–166.

Koopal, L. K., van Riemsdijk, W. H., and Roffey, M. G. (1987). Surface ionization and complexation models: a comparison of methods for determining model parameters. *J. Colloid Interface Sci.* **118**, 117–136.

Koretsky, C. (2000). The significance of surface complexation reactions in hydrologic systems: a geochemist's perspective. *J. Hydrol.* **230**, 127–171.

Koretsky, C. M., Sverjensky, D. A., and Sahai, N. (1998). Surface site types on oxide and silicate minerals based on crystal chemistry: implications for site densities, multi-site adsorption, surface infrared spectroscopy, and dissolution kinetics. *Am. J. Sci.* **298**, 349–438.

Kulik, D. A. (2002a). Sorption modelling by Gibbs energy minimisation: towards a uniform thermodynamic database for surface complexes of radionuclides. *Radiochim. Acta* **90**, 815–832.

Kulik, D. A. (2002b). A Gibbs energy minimization approach to model sorption equilibria at the mineral–water interface: thermodynamic relations for multi-site surface-complexation. *Am. J. Sci.* **302**, 227–279.

Kurdi, F., and Doner, H. E. (1983). Zinc and copper sorption and interaction in soils. *Soil Sci. Soc. Am. J.* **47**, 873–876.

Ladeira, A. C. Q., Ciminelli, V. S. T., Duarte, H. A., Alves, M. C. M., and Ramos, A. Y. (2001). Mechanism of anion retention from EXAFS and density functional calculations: arsenic(V) adsorbed on gibbsite. *Geochim. Cosmochim. Acta* **65**, 1211–1217.

Lumsdon, D. G., Fraser, A. R., Russell, J. D., and Livesey, N. T. (1984). New infrared band assignments for the arsenate ion adsorbed on synthetic goethite (α-FeOOH). *J. Soil Sci.* **35**, 381–386.

Manceau, A., and Charlet, L. (1992). X-ray absorption spectroscopic study of the sorption of Cr(III) at the oxide–water interface. I. Molecular mechanism of Cr(III) oxidation on Mn oxides. *J. Colloid Interface Sci.* **148**, 425–442.

Manceau, A., Nagy, K. L., Spadini, L., and Ragnarsdottir, K. V. (2000). Influence of anionic layer structure of Fe-oxyhydroxides on the structure of Cd surface complexes. *J. Colloid Interface Sci.* **228**, 306–316.

Manning, B. A., and Goldberg, S. (1996). Modeling competitive adsorption of arsenate with phosphate and molybdate on oxide minerals. *Soil Sci. Soc. Am. J.* **60**, 121–131.

Manning, B. A., Fendorf, S. E., and Goldberg, S. (1998). Surface structures and stability of arsenic(III) on goethite. Spectroscopic evidence for inner-sphere complexes. *Environ. Sci. Technol.* **32**, 2383–2388.

McBride, M. B. (1997). A critique of diffuse double layer models applied to colloid and surface chemistry. *Clays Clay Miner.* **45**, 598–608.

McBride, M. B. (1982). Cu^{2+}-adsorption characteristics of aluminum hydroxide and oxyhydroxides. *Clays Clay Miner.* **30**, 21–28.

McBride, M. B., Fraser, A. R., and McHardy, W. J. (1984). Cu^{2+} interaction with microcrystalline gibbsite. Evidence for oriented chemisorbed copper ions. *Clays Clay Miner.* **32**, 12–18.

McKenzie, R. M. (1983). The adsorption of molybdenum on oxide surfaces. *Aust. J. Soil Res.* **21**, 505–513.

Meeussen, J. C. L. (2003). ORCHESTRA: an object-oriented framework for implementing chemical equilibrium models. *Environ. Sci. Technol.* **37**, 1175–1182.

Micera, G., Dallacchio, R., Deiana, S., Gessa, C., Melis, P., and Premoli, A. (1986). Manganese(II)–aluminum hydroxide interaction: an ESR study. *Colloids Surf.* **17**, 395–400.

O'Day, P. A., Parks, G. A., and Brown, G. E. (1994). Molecular structure and binding sites of cobalt(II) surface complexes on kaolinite from x-ray absorption spectroscopy. *Clays Clay Miner.* **42**, 337–355.

O'Day, P. A., Newville, M., Neuhoff, P. S., Sahai, N., and Carroll, S. A. (2000). X-ray absorption spectroscopy of strontium(II) coordination. I. Static and thermal disorder in crystalline, hydrated, and precipitated solids and in aqueous solution. *J. Colloid Interface Sci.* **222**, 184–197.

Papelis, C., Hayes, K. F., and Leckie, J. O. (1988). *HYDRAQL: A Program for the Computation of Chemical Equilibrium Composition of Aqueous Batch Systems Including Surface-Complexation Modeling of Ion Adsorption at the Oxide/Solution Interface,* Tech. Rep. 306, Department of Civil Engineering, Stanford University, Stanford, CA.

Payne, T. E., Davis, J. A., Ochs, M., Olin, M., and Tweed, C. J. (2004). Uranium adsorption on weathered schist—intercomparison of modelling approaches. *Radiochim. Acta* **92**, 651–661.

Peacock, C. L., and Sherman, D. M. (2004a). Copper(II) sorption onto goethite, hematite, and lepidocrocite: a surface complexation model based on ab initio molecular geometries and EXAFS spectroscopy. *Geochim. Cosmochim. Acta* **68**, 2623–2637.

Peacock, C. L., and Sherman, D. M. (2004b). Vanadium(V) adsorption onto goethite (α-FeOOH) at pH 1.5 to 12: a surface complexation model based on ab initio molecular geometries and EXAFS spectroscopy. *Geochim. Cosmochim. Acta* **68**, 1723–1734.

Pierce, M. L., and Moore, C. B. (1980). Adsorption of arsenite on amorphous iron hydroxide from dilute aqueous solution. *Environ. Sci. Technol.* **14**, 214–216.

Randall, S. R., Sherman, D. M., Ragnarsdòttir, K. V., and Collins C. R. (1999). The mechanism of cadmium surface complexation on iron oxyhydroxide minerals. *Geochim. Cosmochim. Acta* **63**, 2971–2987.

Rochester, C. H., and Topham, S. A. (1979a). Infrared study of surface hydroxyl groups on goethite. *J. Chem. Soc. Faraday Trans. I* **75**, 591–602.

Rochester, C. H., and Topham, S. A. (1979b). Infrared study of surface hydroxyl groups on haematite. *J. Chem. Soc. Faraday Trans. I* **75**, 1073–1088.

Roe, A. L., Hayes, K. F., Chisholm-Brause, C. J., Brown, G. E., Parks, G. A., Hodgson, K. O., and Leckie, J. O. (1991). In situ x-ray absorption study of lead ion surface complexes at the goethite–water interface. *Langmuir* **7**, 367–373.

Sahai, N. (2002). Is silica really an anomalous oxide? Surface acidity and aqueous hydrolysis revisited. *Environ. Sci. Technol.* **36**, 445–452.

Sahai, N., and Sverjensky, D. A. (1997a). Evaluation of internally consistent parameters for the triple-layer model by the systematic analysis of oxide surface titration data. *Geochim. Cosmochim. Acta* **61**, 2801–2826.

Sahai, N., and Sverjensky, D. A. (1997b). Solvation and electrostatic model for specific electrolyte adsorption. *Geochim. Cosmochim. Acta* **61**, 2827–2848.

Sahai, N., and Sverjensky, D. A. (1998). GEOSURF: a computer program for modeling adsorption on mineral surfaces from aqueous solution. *Comput. Geosci.* **24**, 853–873.

Sahai, N., Carroll, S. A., Roberts, S., and O'Day, P. A. (2000). X-ray absorption spectroscopy of strontium(II) coordination. II. Sorption and precipitation at kaolinite, amorphous silica, and goethite surfaces. *J. Colloid Interface Sci.* **222**, 198–212.

Schindler, P. W., Fürst, B., Dick, R and Wolf, P. U. (1976). Ligand properties of surface silanol groups. I. Surface complex formation with Fe^{3+}, Cu^{2+}, Cd^{2+}, and Pb^{2+}. *J. Colloid Interface Sci.* **55**, 469–475.

Schudel, M., Behrens, S. H., Holthoff, H., Kretzschmar, R., and Borkovec, M. (1997). Absolute aggregation rate constants of hematite particles in aqueous suspensions: a comparison of two different surface morphologies. *J. Colloid Interface Sci.* **196**, 241–253.

Secor, R. B., and Radke, C. J. (1985). Spillover of the diffuse double layer on montmorillonite particles. *J. Colloid Interface Sci.* **103**, 237–244.

Shuman, L. M. (1975). The effect of soil properties on zinc adsorption by soils. *Soil Sci. Soc. Am. Proc.* **39**, 454–458.

Spadini, L., Manceau, A., Schindler, P. W., and Charlet, L. (1994). Structure and stability of Cd^{2+} surface complexes on ferric oxides. I. Results from EXAFS spectroscopy. *J. Colloid Interface Sci.* **168**, 73–86.

Sposito, G. (1982). On the use of the Langmuir equation in the interpretation of "adsorption" phenomena. II. The "two-surface" Langmuir equation. *Soil Sci. Soc. Am. J.* **46**, 1147–1152.

Sposito, G. (1984). *The Surface Chemistry of Soils*, Oxford University Press, Oxford.

Sprycha, R. (1984). Surface charge and adsorption of background electrolyte ions at anatase/electrolyte interface. *J. Colloid Interface Sci.* **102**, 173–185.

Steele, H. M., Wright, K., Nygren, M. A., and Hillier, I. H. (2000). Interactions of the (001) surface of muscovite with Cu(II), Zn(II), and Cd(II): a computer simulation study. *Geochim. Cosmochim. Acta* **64**, 257–262.

Strawn, D. G., and Sparks, D. L. (1999). The use of XAFS to distinguish between inner- and outer-sphere lead adsorption complexes on montmorillonite. *J. Colloid Interface Sci.* **216**, 257–269.

Strawn, D. G., Scheidegger, A. M., and Sparks, D. L. (1998). Kinetics and mechanisms of Pb(II) sorption and desorption at the aluminum oxide water interface. *Environ. Sci. Technol.* **32**, 2596–2601.

Stumm, W., Kummert, R., and Sigg, L. (1980). A ligand exchange model for the adsorption of inorganic and organic ligands at hydrous oxide interfaces. *Croat. Chem. Acta* **53**, 291–312.

Sturchio, N. C., Chiarello, R. P., Cheng, L., Lyman, P. F., Bedzyk, M. J., Qian, Y., You, H., Yee, D., Geissbuhler, P., Sorenson, L. B., Liang, Y., and Baer, D. R. (1997). Lead adsorption at the calcite–water interface: synchrotron x-ray standing wave and x-ray reflectivity studies. *Geochim. Cosmochim. Acta* **61**, 251–263.

Suarez, D. L., Goldberg, S., and Su, C. (1998). Evaluation of oxyanion adsorption mechanisms on oxides using FTIR spectroscopy and electrophoretic mobility. *Am. Chem. Soc. Symp. Ser.* **715**, 136–178.

Sverjensky, D. A. (1993). Physical surface-complexation models for sorption at the mineral–water interface. *Nature* **364**, 776–780.

Sverjensky, D. A. (2001). Interpretation and prediction of triple-layer model capacitances and the structure of the oxide–electrolyte–water interface. *Geochim. Cosmochim. Acta* **65**, 3643–3655.

Sverjensky, D. A. (2003). Standard states for the activities of mineral surface sites and species. *Geochim. Cosmochim. Acta* **67**, 17–28.

Sverjensky, D. A. (2005). Prediction of surface charge on oxides in salt solutions: revisions for 1 : 1 (M^+L^-) electrolytes. *Geochim. Cosmochim. Acta* **69**, 225–257.

Sverjensky, D. A., and Sahai, N. (1996). Theoretical prediction of single-site surface-protonation equilibrium constants for oxides and silicates in water. *Geochim. Cosmochim. Acta* **60**, 3773–3797.

Tadanier, C., and Eick, M. J. (2002). Formulating the charge distribution multisite surface complexation model using FITEQL. *Soil Sci. Soc. Am. J.* **66**, 1505–1517.

Towle, S. N., Bargar, J. R., Brown, G. E., and Parks, G. A. (1999). Sorption of Cu(II) on metal oxide surfaces. II. Identification of $Co(II)_{(aq)}$ adsorption sites on the (0001) and (1(1) $\bar{0}$2) surfaces of α-Al_2O_3 by grazing incidence XAFS spectroscopy. *J. Colloid Interface Sci.* **217**, 312–321.

Trainor, T. P., Brown, G. E., and Parks, G. A. (2000). Adsorption and precipitation of aqueous Zn(II) on alumina powders. *J. Colloid Interface Sci.* **231**, 359–372.

Trivedi, P., Axe, L., and Tyson, T. A. (2001a). XAS studies of Ni and Zn sorbed to hydrous manganese oxide. *Environ. Sci. Technol.* **35**, 4515–4521.

Trivedi, P., Axe, L., and Tyson, T. A. (2001b). An analysis of zinc sorption to amorphous versus crystalline iron oxides using XAS. *J. Colloid Interface Sci.* **244**, 230–238.

Trivedi, P., Dyer, J. A., and Sparks, D. L. (2003). Lead sorption onto ferrihydrite. 1. A macroscopic and spectroscopic assessment. *Environ. Sci. Technol.* **37**, 908–914.

Turner, M. A., Hendrickson, L. L., and Corey, R. B. (1984). Use of chelating resins in metal adsorption studies. *Soil Sci. Soc. Am. J.* **48**, 763–769.

van der Lee, J., and Lomenech, C. (2004). Towards a common thermodynamic database for speciation models. *Radiochim. Acta* **92**, 811–818.

Veith, J. A., and Sposito, G. (1977). On the use of the Langmuir equation in the interpretation of "adsorption" phenomena. *Soil Sci. Soc. Am. J.* **41**, 697–702.

Venema, P., Hiemstra, T., and van Riemsdijk, W. H. (1996a). Comparison of different site binding models for cation sorption: description of pH dependency, salt dependency, and cation–proton exchange. *J. Colloid Interface Sci.* **181**, 45–59.

Venema, P., Hiemstra, T., and van Riemsdijk, W. H. (1996b). Multisite adsorption of cadmium on goethite. *J. Colloid Interface Sci.* **183**, 515–527.

Venema, P., Hiemstra, T., and van Riemsdijk, W. H. (1997). Interaction of cadmium with phosphate on goethite. *J. Colloid Interface Sci.* **192**, 94–103.

Villalobos, M., Trotz, M. A., and Leckie, J. O. (2003). Variability in goethite surface site density: evidence from proton and carbonate sorption. *J. Colloid Interface Sci.* **268**, 273–287.

Waite, T. D., Davis, J. A., Payne, T. E., Waychunas, G. A., and Xu, N. (1994). Uranium(VI) adsorption to ferrihydrite: application of a surface complexation model. *Geochim. Cosmochim. Acta* **58**, 5465–5478.

Waychunas, G. A., Rea, B. A., Fuller, C. C., and Davis, J. A. (1993). Surface chemistry of ferrihydrite. 1. EXAFS studies of the geometry of coprecipitated and adsorbed arsenate. *Geochim. Cosmochim. Acta* **57**, 2251–2269.

Waychunas, G. A., Fuller, C. C., and Davis, J. A. (2002). Surface complexation and precipitate geometry for aqueous Zn(II) sorption on ferrihydrite. I. X-ray absorption extended fine structure spectroscopy analysis. *Geochim. Cosmochim. Acta* **66**, 1119–1137.

Weng, L., Temminghoff, E. J. M., and van Riemsdijk, W. H. (2001). Contribution of individual sorbents to the control of heavy metal activity in sandy soil. *Environ. Sci. Technol.* **35**, 4436–4443.

Weng, L., Temminghoff, E. J. M., Lofts, S., Tipping, E., and van Riemsdijk, W. H. (2002). Complexation of dissolved organic matter and solubility control of heavy metals in a sandy soil. *Environ. Sci. Technol.* 36, 4804–4810.

Westall, J. C. (1979). *MICROQL. I. A Chemical Equilibrium Program in BASIC. II. Computation of Adsorption Equilibria in BASIC*, Tech. Rep., Swiss Federal Institute of Technology, EAWAG, Dübendorf, Switzerland.

Westall, J. (1980). Chemical equilibrium including adsorption on charged surfaces. *Am. Chem. Soc. Adv. Chem. Ser.* **189**, 33–44.

Yates, D. E. (1975). The Structure of the oxide/aqueous electrolyte interface. Ph.D. dissertation, University of Melbourne, Melbourne, VIC, Australia.

Yates, D. E., Levine, S., and Healy, T. W. (1974). Site-binding model of the electrical double layer at the oxide/water interface. *J. Chem. Soc. Faraday Trans. I* **70**, 1807–1818.

Yoon, R. H., Salman, T., and Donnay, G. (1979). Predicting points of zero charge of oxides and hydroxides. *J. Colloid Interface Sci.* **70**, 483–493.

Zhang Z., Fenter, P., Cheng, L., Sturchio, N. C., Bedzyk, M. J., Predota, M., Bandura, A., Kubicki, J. D., Lvov, S. N., Cummings, P. T., Chioalvo, A. A., Ridley, M. K., Bénézeth, P., Anovitz, L., Palmer, D. A., Machesky, M. L., and Wesolowski, D. J. (2004). Ion adsorption at the rutile–water interface: linking molecular and macroscopic properties. *Langmuir* **20**, 4954–4969.